Eur. Phys. J. C (2022) 82:954
https://doi.org/10.1140/epjc/s10052-022-10928-3

THE EUROPEAN PHYSICAL JOURNAL C

Check for updates

Regular Article - Theoretical Physics

Leptonic anomalous magnetic and electric dipole moments in the CP-violating NMSSM with and without inverse seesaw mechanism

Thi Nhung Dao[1,a], **Duc Ninh Le**[1,b], **Margarete Mühlleitner**[2,c]

[1] Faculty of Fundamental Sciences, PHENIKAA University, Hanoi 12116, Vietnam
[2] Institute for Theoretical Physics, Karlsruhe Institute of Technology, 76128 Karlsruhe, Germany

Received: 4 August 2022 / Accepted: 15 October 2022
© The Author(s) 2022

Abstract The new results on the muon anomalous magnetic moment (AMM) published by Fermilab in 2021 did not lead to a reduction of its long-pending deviation from the Standard Model (SM) value by more than 4σ. The explanation of this discrepancy by adding new particles to the theory puts many new physics models under tension when combined with the null results of the LHC direct searches for new particles. In this paper, we investigate the CP-violating Next-to-Minimal Supersymmetric extension of the SM (NMSSM) with and without an inverse seesaw mechanism. We compute the one-loop supersymmetric contributions to the AMM and the two-loop Barr–Zee-type diagrams with effective Higgs couplings to photons for the leptonic electric dipole moments (EDMs). The effects of the extended (s)neutrino sector on the muon AMM and on the mass of the SM-like Higgs boson can be significant. Complex phases can have an important impact on the AMM. On the other hand, the stringent limits from the EDMs on the complex phases have to be taken into account. Our calculations have been implemented in the Fortran codes `NMSSMCALC` and `NMSSMCALC-nuSS` which are publicly available. Besides the leptonic AMMs and EDMs, these programs can compute the Higgs boson masses and mixings, together with Higgs boson decay widths and branching ratios taking into account the most up-to-date higher-order corrections in the NMSSM with and without inverse seesaw mechanism.

1 Introduction

At the beginning of 2021, the Fermilab Muon $g-2$ collaboration reported their first result [1] of the muon anomalous magnetic moment (AMM) $a_\mu \equiv (g_\mu - 2)/2$,

$$a_\mu^{\text{FNAL}} = (11659204.0 \pm 5.4) \times 10^{-10}, \tag{1}$$

which is consistent with the previous measurement by the E821 experiment at BNL with [2]

$$a_\mu^{\text{BNL}} = (11659208.9 \pm 6.3) \times 10^{-10}. \tag{2}$$

The combined result, $a_\mu^{\text{exp}} = (11659206.1 \pm 4.1) \times 10^{-10}$ compared with the theoretical prediction of the Standard Model (SM) [3]

$$a_\mu^{\text{SM}} = (11659181.0 \pm 4.3) \times 10^{-10} \tag{3}$$

leads to a deviation,

$$\Delta a_\mu \equiv a_\mu^{\text{exp}} - a_\mu^{\text{SM}} = (25.1 \pm 5.9) \times 10^{-10}, \tag{4}$$

at the 4.2σ level. The SM result consists of the pure QED, electroweak and hadronic contributions. The pure QED contribution has been evaluated up to $\mathcal{O}(\alpha^5)$ [4] with negligible uncertainty, the electroweak correction has been computed up to leading three-loop order with less than one percent of uncertainty, see [3] and references therein, and is suppressed by the ratio m_μ^2/M_W^2 where m_μ and M_W are the mass of the muon and the W boson, respectively. The largest uncertainty comes from the hadronic contributions which are calculated using non-perturbative methods. Very recently, the hadronic light-by-light contribution was computed by using lattice QCD [5] and slightly reduced the significance of the anomaly.

The anomaly is tantalizing in view of new physics at the weak scale [6]. Most of the models which try to explain this discrepancy tend to extend the electroweak sector to include additional corrections, a_μ^{new}. In the Minimal Supersymmetric extension of the SM (MSSM), besides the two Higgs doublets H_u and H_d, there are additional fields given by the superpartners of the muons, Higgs bosons and gauge bosons that

[a] e-mail: nhung.daothi@phenikaa-uni.edu.vn (corresponding author)
[b] e-mail: ninh.leduc@phenikaa-uni.edu.vn
[c] e-mail: margarete.muehlleitner@kit.edu

Published online: 27 October 2022

interact directly with the muons. They enter the one-loop diagrams that contribute to $a_\mu^{\rm new}$. The new contributions depend on the ratio m_μ^2/M_S^2, where M_S represents the mass scale of the supersymmetric (SUSY) particles and the muon Yukawa coupling $y_\mu = \sqrt{2}m_\mu/(v\cos\beta)$. Here v denotes the vacuum expectation value given in terms of the two vacuum expectation values v_u and v_d of the two Higgs doublets H_u and H_d, respectively, $v = \sqrt{v_u^2 + v_d^2}$, and $\tan\beta \equiv v_u/v_d$. The new contribution $a_\mu^{\rm new}$ can be significant when M_S is small and/or $\tan\beta$ becomes large. The non-observation of SUSY particles at the LHC, however, pushes the SUSY mass scale M_S to the TeV range. Moreover, the Higgs signals measured at the LHC require the SM-like Higgs couplings to be close to the ones of the SM, and therefore $\tan\beta$ should not be large. Furthermore, the SM-like Higgs should be the h_u-dominated Higgs boson so that it couples with a SM-like coupling to the top quarks. These requirements constrain the value of $a_\mu^{\rm new}$.

The Next-to-Minimal Supersymmetric SM (NMSSM) contains an additional complex singlet superfield [7–22]. Its scalar component can mix with the scalar components of the two Higgs doublet superfields which results in five neutral scalar Higgs boson states. Although the LHC Higgs data has pushed the mass of the dominantly doublet-like scalar/pseudoscalar Higgs states, h_d/a_d, into the TeV range it still allows for the singlet-like Higgs boson masses to be in the GeV range. This makes the NMSSM an interesting candidate for Higgs physics beyond the SM. As for the muon AMM, one expects a similar contribution from the electroweakino sector as in the MSSM. A noticeable difference may come from the contribution of a singlet-like Higgs boson with a mass of a few GeV. However, the one and two-loop light Higgs contributions are of opposite sign and therefore interfere destructively as shown in [23,24]. When the (s)neutrino sector of the NMSSM is extended to include six singlet leptonic superfields ($\hat{N}_i$, $\hat{X}_i$, $i = 1, 2, 3$), the three very small neutrino masses can then be generated through the inverse seesaw mechanism [25–27]. This extension of the NMSSM was first discussed in [28]. The h_u-like Higgs boson now has interactions with the left-handed doublet neutrinos ν_L^i and the new singlet fermionic components N^i, and also with their scalar partners, that are proportional to the neutrino Yukawa couplings. These can induce new one-loop contributions to the Higgs boson masses as shown in [29–31]. This extension gives rise to the mixing between left-handed doublet sneutrinos $\tilde{\nu}_L^i$ with the right-handed ones so that the sneutrino masses can be rather light. This opens the possibility that the lightest sneutrinos can be a feasible Dark Matter candidate, as shown in [32,33]. The extended sneutrino sector also gives rise to a new one-loop contribution to the AMM of the charged leptons, as shown in [34,35].

In this study we compute and subsequently discuss the full one-loop SUSY contributions to the leptonic AMM and electric dipole moment (EDM) in the NMSSM and a variant of the NMSSM with inverse seesaw mechanism (abbreviated as NMSSM-nuSS) taking into account non-vanishing CP-violating phases. We further include contributions from the two-loop Barr–Zee-type diagrams with effective $h\gamma\gamma$ couplings. We show in this study the correlation between the impacts of the extended (s)neutrino sector on the muon AMM and on the loop-corrected h_u-like Higgs boson mass. The impacts can be significant simultaneously. In the regions where a positive SUSY contribution to the muon AMM is necessary to explain the anomaly, the one-loop contributions from the extended (s)neutrino sector to the h_u-like Higgs boson mass can become negative since the sneutrino contributions dominate over the neutrino contributions. We also study the effects of the complex phases on the muon AMM in both models. All these contributions to the AMM and to the EDM of the charged leptons have been implemented in our two published Fortran codes `NMSSMCALC` [36–40] and `NMSSMCALC-nuSS` [31] which compute the Higgs boson masses and mixings, together with Higgs boson decay widths and branching ratios taking into account the most up-to-date higher-order corrections. The codes can be downloaded from the url:

https://www.itp.kit.edu/~maggie/NMSSMCALC/

and

https://www.itp.kit.edu/~maggie/NMSSMCALC-nuSS/

The paper is organised as follows. Section 2 introduces the models and our notations. In Sect. 3 we present our computation and analytical expressions of the one-loop and two-loop contributions to the leptonic AMM and EDM. The set-up of the calculation and the numerical analysis are given in Sect. 4. We conclude in Sect. 5.

2 The complex NMSSM and the NMSSM with inverse seesaw mechanism

The difference between the complex NMSSM and the complex NMSSM with inverse seesaw mechanism manifests itself mainly in the neutrino and sneutrino sectors. We start with a short description of the complex NMSSM to introduce the model parameters. We follow the same notation which has been used in our previous studies [36–40]. The complex NMSSM superpotential is given by ($i, j = 1, 2$)

$$\begin{aligned}\mathcal{W}_{\rm NMSSM} = \epsilon_{ij}[y_e \hat{H}_d^i \hat{L}^j \hat{E}^c + y_d \hat{H}_d^i \hat{Q}^j \hat{D}^c - y_u \hat{H}_u^i \hat{Q}^j \hat{U}^c] \\ - \epsilon_{ij}\lambda \hat{S} \hat{H}_d^i \hat{H}_u^j + \frac{1}{3}\kappa \hat{S}^3, \end{aligned} \tag{5}$$

with the quark and leptonic superfields $\hat{Q}$, $\hat{U}$, $\hat{D}$, $\hat{L}$, $\hat{E}$, and the Higgs doublet superfields $\hat{H}_d$, $\hat{H}_u$ and the singlet super-

field $\hat{S}$ and the totally antisymmetric tensor $\epsilon_{12} = \epsilon^{12} = 1$. Charge conjugated fields are denoted by the superscript c. Color and generation indices have been suppressed for the sake of clarity. The Yukawa couplings y_u, y_d and y_e are taken as diagonal 3×3 matrices in the flavour space. The coupling parameters λ and κ are complex numbers in the CP-violating NMSSM. The soft SUSY-breaking Lagrangian reads

$$\begin{aligned}
&\mathcal{L}_{\text{soft,NMSSM}} \\
&= -m_{H_d}^2 H_d^\dagger H_d - m_{H_u}^2 H_u^\dagger H_u - m_{\tilde{Q}}^2 \tilde{Q}^\dagger \tilde{Q} - m_{\tilde{L}}^2 \tilde{L}^\dagger \tilde{L} \\
&\quad - m_{\tilde{u}_R}^2 \tilde{u}_R^* \tilde{u}_R - m_{\tilde{d}_R}^2 \tilde{d}_R^* \tilde{d}_R \\
&\quad - m_{\tilde{e}_R}^2 \tilde{e}_R^* \tilde{e}_R - (\epsilon_{ij}[y_e A_e H_d^i \tilde{L}^j \tilde{e}_R^* + y_d A_d H_d^i \tilde{Q}^j \tilde{d}_R^* \\
&\quad - y_u A_u H_u^i \tilde{Q}^j \tilde{u}_R^*] + \text{h.c.}) \\
&\quad - \frac{1}{2}(M_1 \tilde{B}\tilde{B} + M_2 \tilde{W}_j \tilde{W}_j + M_3 \tilde{G}\tilde{G} + \text{h.c.}) \\
&\quad - m_S^2 |S|^2 + \left(\epsilon_{ij} \lambda A_\lambda S H_d^i H_u^j - \frac{1}{3}\kappa A_\kappa S^3 + \text{h.c.}\right). \qquad (6)
\end{aligned}$$

The $H_{u,d}$ are two scalar Higgs doublets, S a scalar singlet field, $\tilde{Q}$ scalar squark doublets, $\tilde{L}$ scalar slepton doublets, $\tilde{u}_R$ and $\tilde{d}_R$ scalar squark singlet fields, and $\tilde{e}_R$ a scalar slepton singlet field. The soft SUSY-breaking gaugino mass parameters M_k ($k = 1, 2, 3$) of the bino, wino and gluino fields $\tilde{B}$, $\tilde{W}_l$ ($l = 1, 2, 3$) and $\tilde{G}$ as well as the soft SUSY-breaking trilinear couplings A_x ($x = \lambda, \kappa, u, d, e$) are complex in the CP-violating NMSSM.

After electroweak symmetry breaking, the Higgs boson fields can be expanded around their vacuum expectation values (VEVs) v_u, v_d, and v_s, respectively,

$$\begin{aligned}
H_d &= \begin{pmatrix} \frac{v_d + h_d + i a_d}{\sqrt{2}} \\ h_d^- \end{pmatrix}, \quad H_u = e^{i\varphi_u} \begin{pmatrix} h_u^+ \\ \frac{v_u + h_u + i a_u}{\sqrt{2}} \end{pmatrix}, \\
S &= \frac{e^{i\varphi_s}}{\sqrt{2}}(v_s + h_s + i a_s), \qquad (7)
\end{aligned}$$

with the CP-violating phases $\varphi_{u,s}$ and we obtain the tree-level spectrum of the Higgs sector. The relation to the SM VEV $v \approx 246.22$ GeV is given by

$$v^2 = v_u^2 + v_d^2 \qquad (8)$$

and we define the mixing angle $\tan\beta$ as

$$\tan\beta = \frac{v_u}{v_d}. \qquad (9)$$

The effective μ parameter is given by

$$\mu_{\text{eff}} = \frac{\lambda v_s e^{i\varphi_s}}{\sqrt{2}}. \qquad (10)$$

Besides the gauge bosons, quarks, charged leptons, and three left-handed neutrino fields as in the SM, we have an extended Higgs spectrum and new SUSY particles, in particular:

- The CP-even and CP-odd Higgs interaction states $(h_{d,u,s}, a_{u,d,s})$ mix to form five CP indefinite Higgs mass eigenstates h_i ($i = 1, \ldots, 5$), with their masses per convention ordered as $m_{h_1} < m_{h_2} < m_{h_3} < m_{h_4} < m_{h_5}$, and one neutral Goldstone boson G^0. We use a two-fold rotation to rotate from the interaction to the mass eigenstates,

$$\begin{aligned}
&(h_d, h_u, h_s, a, a_s, G^0)^T \\
&\quad = \mathcal{R}^G(\beta)\,(h_d, h_u, h_s, a_d, a_u, a_s)^T, \qquad (11) \\
&(h_1, h_2, h_3, h_4, h_5, G^0)^T \\
&\quad = \mathcal{R}^H\,(h_d, h_u, h_s, a, a_s, G^0)^T, \qquad (12)
\end{aligned}$$

  where the first rotation matrix $\mathcal{R}^G$ with one rotation angle β singles out the neutral Goldstone boson and the second rotation matrix $\mathcal{R}^H$ rotates the five interaction states (h_d, h_u, h_s, a, a_s) to the five mass eigenstates $(h_1, h_2, h_3, h_4, h_5)$.
- The charged Higgs interaction states $h_d^\pm$, $h_u^\pm$ constitute the charged Higgs bosons $H^\pm$ with mass $M_{H^\pm}$ and the charged Goldstone bosons $G^\pm$.
- The fermionic partners of the neutral Higgs bosons, the neutral higgsinos $\tilde{H}_u$, $\tilde{H}_d$ and the singlino $\tilde{S}$, mix with the neutral gauginos $\tilde{B}$ and $\tilde{W}^3$, resulting in five neutralinos denoted as $\tilde{\chi}_i^0$, ($i = 1, \ldots, 5$). The mass ordering of the $\tilde{\chi}_i^0$ is chosen as $m_{\tilde{\chi}_1^0} \leq \cdots \leq m_{\tilde{\chi}_5^0}$ and the rotation matrix N transforms the fields $(\tilde{B},\ \tilde{W}^3,\ \tilde{H}_d,\ \tilde{H}_u, \tilde{S})^T$ into the mass eigenstates.
- The two chargino mass eigenstates,

$$\tilde{\chi}_i^+ = \begin{pmatrix} \tilde{\chi}_{L_i}^+ \\ \tilde{\chi}_{R_i}^- \end{pmatrix}, \quad i = 1, 2, \qquad (13)$$

  are obtained from the rotation of the interaction states, given by the charged Higgsinos $\tilde{H}_d^\pm$, $\tilde{H}_u^\pm$ and the charged gauginos $\tilde{W}^\pm$, to the mass eigenstates. This is done by a bi-unitary transformation with the two 2×2 unitary matrices V^χ and U^χ,

$$\tilde{\chi}_L^+ = V^\chi(\tilde{W}^+, \tilde{H}_u^+)^T, \quad \tilde{\chi}_R^- = U^\chi(\tilde{W}^-, \tilde{H}_d^-)^T. \qquad (14)$$

- The scalar partners of the left- and right-handed up-type quarks are denoted by $\tilde{u}_{L/R}^i$, of the down-type quarks by $\tilde{d}_{L/R}^i$, and of the charged leptons by $\tilde{l}_{L/R}^i$ ($i = 1, 2, 3$). We do not include flavor mixing. Within each flavour the left- and right-handed scalar fermions with same electric charge mix and they are rotated to the mass eigenstates by a unitary matrix $U^{\tilde{f}}$.
- There are three scalar partners of the left-handed neutrinos, denoted as $\tilde{\nu}_i$ ($i = 1, 2, 3$) with their masses given by

$$m^2_{\tilde{\nu}_i} = \frac{1}{2} M_Z^2 c_{2\beta} + m^2_{\tilde{L}_i}, \tag{15}$$

where the short hand notation $c_x \equiv \cos(x), s_x \equiv \sin(x), t_x \equiv \tan(x)$ is used in this paper and the second term comes from the soft SUSY-breaking Lagrangian in (6).

The complex NMSSM with inverse seesaw mechanism is obtained from the complex NMSSM by including six gauge-singlet chiral superfields $\hat{N}_i, \hat{X}_i$ $(i = 1, 2, 3)$ that carry lepton number. We follow the same notation as in our previous investigation of the loop corrections to the neutral Higgs boson masses presented in [31]. The superpotential of the model reads $(i, j = 1, 2)$

$$\begin{aligned} \mathcal{W}_{\text{NMSSM-nuSS}} = \mathcal{W}_{\text{NMSSM}} &- y_\nu \epsilon_{ij} \hat{H}_u^i \hat{L}^j \hat{N}^c \\ &+ \lambda_X \hat{S} \hat{X} \hat{X} + \mu_X \hat{X} \hat{N}^c, \end{aligned} \tag{16}$$

where the neutrino Yukawa coupling y_ν and the coupling λ_X are 3×3 complex matrices in general, and the superscript c denotes the charge conjugation. The $\lambda_X \hat{S} \hat{X} \hat{X}$ term violates the lepton number by two units, see Ref. [31], therefore we require λ_X to be extremely small. The 3×3 matrix μ_X is the only parameter with the dimension of mass in the superpotential. It, however, does not participate in the spontaneous electroweak symmetry breaking process and therefore does not give rise to the well known μ-problem in the MSSM. Furthermore, the $\mu_X \hat{X} \hat{N}^c$ term preserves lepton number as discussed in [31], hence μ_X can be of the order of the SUSY conserving mass scale and is naturally large. This is essential for the seesaw mechanism. The soft SUSY-breaking NMSSM Lagrangian respecting the gauge symmetries and the global $\mathbb{Z}_3$ symmetry reads (the assignment of the $\mathbb{Z}_3$ charges is provided in [31])

$$\begin{aligned} \mathcal{L}^{\text{soft}}_{\text{NMSSM-nuSS}} = \mathcal{L}^{\text{soft}}_{\text{NMSSM}} &+ (\epsilon_{ab} y_\nu A_\nu H_u^a \tilde{L}^b \tilde{N}^* \\ &+ \lambda_X A_X S \tilde{X} \tilde{X} + \mu_X B_{\mu_X} \tilde{X} \tilde{N}^* + h.c.) \\ &- \tilde{m}_X^2 \left| \tilde{X} \right|^2 - \tilde{m}_N^2 \left| \tilde{N} \right|^2, \end{aligned} \tag{17}$$

which introduces the soft SUSY-breaking trilinear couplings A_ν, A_X, the soft SUSY-breaking masses $\tilde{m}_X^2, \tilde{m}_N^2$, and the soft SUSY-breaking bilinear mass B_{μ_X}.

In the neutral leptonic sector, the three left-handed neutrinos ν_{L_i} mix with the six leptonic component fields of the six singlet superfields $\hat{N}_i^c, \hat{X}_i, i = 1, 2, 3$, and the mass term in the Lagrangian reads

$$\mathcal{L}^\nu_{\text{mass}} = -\frac{1}{2} \begin{pmatrix} \nu_L & N^c & X \end{pmatrix} M^\nu_{\text{ISS}} \begin{pmatrix} \nu_L \\ N^c \\ X \end{pmatrix}, \tag{18}$$

where the mixing mass matrix is given by

$$M^\nu_{\text{ISS}} = \begin{pmatrix} 0 & M_D & 0 \\ M_D^T & 0 & \mu_X \\ 0 & \mu_X^T & M_X \end{pmatrix}, \tag{19}$$

where blocks M_D, μ_X and M_X are 3×3 matrices with μ_X defined in Eq. (16) and

$$M_D = \frac{v_u e^{i\varphi_u}}{\sqrt{2}} y_\nu, \quad M_X = \frac{v_s e^{i\varphi_s}}{\sqrt{2}} (\lambda_X + \lambda_X^T). \tag{20}$$

Diagonalizing the neutrino mass matrix with a unitary rotation matrix U^ν, one obtains nine neutrino mass eigenstates with their masses m_{ν_i} $(i = 1, \ldots, 9)$ being sorted in ascending order. By exploiting the fact that all matrix elements of M_D and M_X are much smaller than the eigenvalues of μ_X, the 3×3 light neutrino mass matrix can be expressed at leading order as

$$M_{\text{light}} = M_D M_N^{-1} M_D^T, \quad \text{with } M_N = \mu_X M_X^{-1} \mu_X^T, \tag{21}$$

and then can be diagonalized by the Pontecorvo–Maki–Nakagawa–Sakata (PMNS) matrix U_{PMNS},

$$U^*_{\text{PMNS}} M_{\text{light}} U^\dagger_{\text{PMNS}} = m_\nu, \quad m_\nu = \text{diag}(m_{\nu_1}, m_{\nu_2}, m_{\nu_3}). \tag{22}$$

In order to reproduce the light neutrino oscillation data, two different parameterizations have been considered. In the so-called Casas–Ibarra parameterization [41], M_D is computed from the relation

$$\begin{aligned} M_D &= U^T_{\text{PMNS}} \sqrt{m_\nu} R \sqrt{\mathcal{M}_N} V_\nu, \\ \mathcal{M}_N &= \text{diag}(M_{N_1}, M_{N_2}, M_{N_3}) = V_\nu^* M_N V_\nu^\dagger, \end{aligned} \tag{23}$$

with R being a complex orthogonal matrix and V_ν a unitary matrix diagonalizing M_N. The y_ν are then obtained from (20). The other possibility is to use the μ_X-parameterization [42] in which M_X is computed from the relation

$$M_X = \mu_X^T M_D^{-1} U^*_{\text{PMNS}} m_\nu U^\dagger_{\text{PMNS}} M_D^{T,-1} \mu_X, \tag{24}$$

where M_D is calculated from the input y_ν.

In the sneutrino sector, each sneutrino field is split up into its CP-even and CP-odd components as

$$\tilde{\nu} = \frac{1}{\sqrt{2}} (\tilde{\nu}_+ + i \tilde{\nu}_-), \tag{25}$$

$$\tilde{N}^* = \frac{1}{\sqrt{2}} \left(\tilde{N}_+ + i \tilde{N}_- \right), \tag{26}$$

$$\tilde{X} = \frac{1}{\sqrt{2}} \left(\tilde{X}_+ + i \tilde{X}_- \right). \tag{27}$$

The mass term in the basis $\psi = (\tilde{\nu}_+, \tilde{N}_+, \tilde{X}_+, \tilde{\nu}_-, \tilde{N}_-, \tilde{X}_-)^T$ (generation indices are suppressed) is given by

$$\mathcal{L} = \frac{1}{2} \psi^T M_{\tilde{\nu}} \psi, \tag{28}$$

where the mass matrix $M_{\tilde{\nu}}$ is an 18×18 symmetric matrix that can be found in Appendix A. An orthogonal matrix $U_{\tilde{\nu}}$ can be used to obtain the masses of the sneutrinos as

$$\text{diag}\left(m^2_{\tilde{n}_1}, \ldots, m^2_{\tilde{n}_{18}}\right) = U_{\tilde{\nu}} M_{\tilde{\nu}} U_{\tilde{\nu}}{}^T, \tag{29}$$

where their mass values are ordered as $m^2_{\tilde{n}_1} \leq \cdots \leq m^2_{\tilde{n}_{18}}$.

3 SUSY contributions to the leptonic AMM and EDM

The SUSY contributions to the leptonic AMM a_l and EDM d_l ($l = e, \mu, \tau$) can be calculated in perturbation theory by considering the matrix element decomposed into a relativistic covariant form,

$$\begin{aligned}
&\langle l(p_2)|j^\mu(q)|l(p_1)\rangle \\
&= -ie\bar{u}(p_2)\Bigg[\left(\gamma^\mu - \frac{\not{q} q^\mu}{q^2}\right)(\bar{F}_L(q^2)P_L + \bar{F}^*_L(q^2)P_R) \\
&\quad + \frac{i\sigma^{\mu\nu}q_\nu}{2m_l}(F_L(q^2)P_L + F^*_L(q^2)P_R) \\
&\quad + \frac{q_\mu}{m_l}(\bar{\bar{F}}_L(q^2)P_L + \bar{\bar{F}}^*_L(q^2)P_R)\Bigg]u(p_1)
\end{aligned} \tag{30}$$

where $\sigma^{\mu\nu} = \frac{i}{2}[\gamma^\mu, \gamma^\nu]$, $P_{L/R} = \frac{1 \mp \gamma_5}{2}$, $q = p_2 - p_1$, m_l is the lepton mass and $u(p)$ denotes the Dirac spinor. The form factors F_L, $\bar{F}_L$, $\bar{\bar{F}}_L$ are functions of q^2 and other parameters of the model. The operator $\sigma^{\mu\nu}q_\nu$ is called dipole matrix operator. In the static limit ($q^\mu \to 0$) we have [43]:

$$a_l = \text{Re}[F_L(0)], \quad d_l = \frac{e}{2m_l}\text{Im}[F_L(0)]. \tag{31}$$

In our computation we will use this generic form for both the AMM and EDM keeping all possible complex phases.

3.1 One-loop contributions

It is well known that the contributions to the dipole matrix $\sigma^{\mu\nu}q_\nu$ require a chirality flip. Therefore contributions to $F_L(0)$ are proportional either to the mass of the external lepton or to the masses of the fermions running in the loop diagrams. In Fig. 1, we present all one-loop diagrams which contribute to $F_L(0)$ in the NMSSM-nuSS. Diagrams with neutral or charged Goldstone bosons occur explicitly because we work in the Feynman–'t Hooft gauge. The diagrams 1 and 2 are the same as in the SM. The diagram with the photon exchange belongs to the QED contribution and the diagrams with Z and G^0 belong to the weak contribution. We calculated these diagrams and recovered the results quoted in the literature, see for example [43] and references therein. Since we do not account them in a_l^{new} we do not present their explicit expressions here and will not mention them any more. The diagrams 3–6 belong to the W contribution. In the SM, neutrinos are purely left-handed and massless while in the NMSSM-nuSS we have three light active neutrinos and six sterile neutrinos. We denote the difference between the NMSSM-nuSS and the SM contributions with respect to the W diagrams as

$$F_L^{\text{new},W} = F_L^{\text{NM},W} - F_L^{\text{SM},W} \tag{32}$$

where ($l = e, \mu, \tau$)

$$\begin{aligned}
F_L^{\text{NM},W} &= -\frac{m_l^2}{4\pi^2 v^2}\sum_{i=1}^{9}\Bigg[\frac{1}{2}v^2 s_\beta^2\left|\sum_{k=1}^{3}(U^{\nu\,*}_{i(k+3)}y^\nu_{lk})\right|^2 \\
&\quad \times \left(C_2^{W,\nu_i} + C_{12}^{W,\nu_i} + C_{22}^{W,\nu_i}\right) \\
&\quad + \frac{1}{\sqrt{2}}s_\beta v m_{\nu_i} U^{\nu\,*}_{il} e^{i\varphi_u}\sum_{k=1}^{3}(U^{\nu\,*}_{i(k+3)}y^\nu_{lk}) \\
&\quad \times \left(C_0^{W,\nu_i} + C_1^{W,\nu_i} + C_2^{W,\nu_i}\right) \\
&\quad + M_W^2|U^\nu_{il}|^2\left(-2C_1^{W,\nu_i} + 2C_{12}^{W,\nu_i} + 2C_{22}^{W,\nu_i}\right) \\
&\quad + m_l^2|U^\nu_{il}|^2\left(C_1^{W,\nu_i} + C_{12}^{W,\nu_i} + C_{11}^{W,\nu_i}\right)\Bigg]
\end{aligned} \tag{33}$$

and

$$\begin{aligned}
F_L^{\text{SM},W} &= -\frac{m_l^2}{4\pi^2 v^2}\Bigg[M_W^2\left(-2C_1^{W,\nu} + 2\tilde{C}_{12}^{W,\nu} + 2C_{22}^{W,\nu}\right) \\
&\quad + m_l^2\left(C_2^{W,\nu} + C_{12}^{W,\nu} + C_{22}^{W,\nu}\right)\Bigg].
\end{aligned} \tag{34}$$

Note that we have introduced the abbreviations $C^{x,y}_{i\ldots}$ for the one-loop three-point integral coefficients which will be

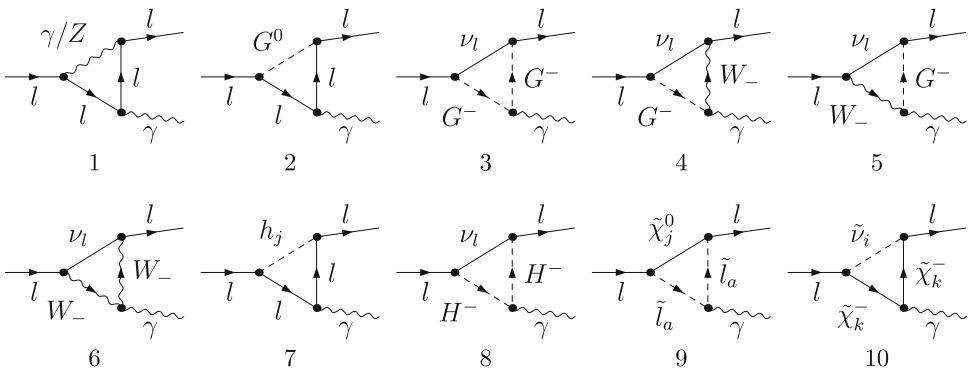

Fig. 1 Generic one-loop Feynman diagrams contributing to the dipole matrix form factor

defined at the end of this section. Expanding $F_L^{\mathrm{SM},W}$ with respect to m_l/M_W we obtained the first term in the expansion in accordance with the well-known result in the literature, see for example [43] and references therein,

$$a_l^{\mathrm{SM},W} = \frac{\sqrt{2}G_\mu m_l^2}{16\pi^2}\frac{10}{3}, \tag{35}$$

where G_μ is the Fermi constant of the muon. While $F_L^{\mathrm{SM},W}$ is real in the SM, $F_L^{\mathrm{NM},W}$ can be complex. In the NMSSM without inverse seesaw mechanism, the neutrino sector is identical to the one of the SM, therefore $F_L^{\mathrm{new},W}$ vanishes. The neutral Higgs boson contribution arises from diagram 7. In our model there are five neutral Higgs bosons while in the SM there is only one neutral state. We denote the new contribution from the neutral Higgs bosons as

$$F_L^{\mathrm{new},H} = F_L^{\mathrm{NM},H} - F_L^{\mathrm{SM},H}, \tag{36}$$

where

$$\begin{aligned} F_L^{\mathrm{NM},H} = \frac{m_l^4}{8\pi^2 v^2}\sum_{j=1}^{5}\Bigg[&\frac{(\mathcal{R}_{j1}^H)^2}{c_\beta^2}\left(2C_1^{h_j,l}+2C_2^{h_j,l}\right.\\ &\left.+C_{11}^{h_j,l}+2C_{12}^{h_j,l}+C_{22}^{h_j,l}\right)\\ &\times t_\beta^2(\mathcal{R}_{j4}^H)^2\left(C_{11}^{h_j,l}+2C_{12}^{h_j,l}+C_{22}^{h_j,l}\right)\\ &+2it_\beta\frac{\mathcal{R}_{j1}^H\mathcal{R}_{j4}^H}{c_\beta}\left(C_1^{h_j,l}+C_2^{h_j,l}\right)\Bigg] \end{aligned} \tag{37}$$

and

$$\begin{aligned} F_L^{\mathrm{SM},H} = \frac{m_l^4}{8\pi^2 v^2}\Bigg[&2C_1^{H_{\mathrm{SM}},l}+2C_2^{H_{\mathrm{SM}},l}+C_{11}^{H_{\mathrm{SM}},l}\\ &+2C_{12}^{H_{\mathrm{SM}},l}+C_{22}^{H_{\mathrm{SM}},l}\Bigg]. \end{aligned} \tag{38}$$

From (37) and (38) it is clear that the Higgs contribution is suppressed by a factor of m_l^2/M_W^2 compared to the W and Z contributions. The last three diagrams 8, 9, and 10 do not appear in the SM. They give rise to the charged Higgs, neutralino and chargino contributions. Our calculations lead to the following results

$$\begin{aligned} F_L^{\mathrm{NM},H^\pm} = -\frac{m_l^2}{16\pi^2}\sum_{i=1}^{9}\Bigg[&2c_\beta^2\left|\sum_{k=1}^{3}(U_{i(k+3)}^{\nu\,*}y_{lk}^{\nu})\right|^2\\ &\times(C_2^{H^\pm,\nu_i}+C_{12}^{H^\pm,\nu_i}+C_{22}^{H^\pm,\nu_i})\\ &-\frac{2^{3/2}e^{i\varphi_u}m_{\nu_i}s_\beta U_{il}^{\nu\,*}}{v}\sum_{k=1}^{3}(U_{i(k+3)}^{\nu\,*}y_{lk}^{\nu})\\ &\times(C_0^{H^\pm,\nu_i}+C_1^{H^\pm,\nu_i}+C_2^{H^\pm,\nu_i})\\ &+\frac{4m_l^2}{v^2}\left|U_{il}^{\nu}\right|^2 t_\beta^2(C_1^{H^\pm,\nu_i}+C_{12}^{H^\pm,\nu_i}+C_{11}^{H^\pm,\nu_i})\Bigg], \end{aligned} \tag{39}$$

$$\begin{aligned} F_L^{\mathrm{NM},\tilde{\chi}^\pm} = \frac{m_l}{8\pi^2}\sum_{i=1}^{18}\sum_{j=1}^{2}\Bigg[&m_l\left(\left|g^L_{l\tilde{\chi}_j^-\tilde{\nu}_i}\right|^2+\left|g^R_{l\tilde{\chi}_j^-\tilde{\nu}_i}\right|^2\right)\\ &\times\left(C_1^{\tilde{\chi}_j^\pm,\tilde{\nu}_i}+C_{12}^{\tilde{\chi}_j^\pm,\tilde{\nu}_i}+C_{11}^{\tilde{\chi}_j^\pm,\tilde{\nu}_i}\right)\\ &+m_{\tilde{\chi}_j^\pm}g^{R*}_{l\tilde{\chi}_j^-\tilde{\nu}_i}g^L_{l\tilde{\chi}_j^-\tilde{\nu}_i}\left(C_1^{\tilde{\chi}_j^\pm,\tilde{\nu}_i}+C_2^{\tilde{\chi}_j^\pm,\tilde{\nu}_i}\right)\Bigg], \end{aligned} \tag{40}$$

$$\begin{aligned} F_L^{\mathrm{NM},\tilde{\chi}^0} = \frac{m_l}{8\pi^2}\sum_{a=1}^{2}\sum_{k=1}^{5}\Bigg[&-m_l\left(\left|g^L_{l\tilde{\chi}_k^0\tilde{l}_a}\right|^2+\left|g^R_{l\tilde{\chi}_k^0\tilde{l}_a}\right|^2\right)\\ &\times\left(C_1^{\tilde{\chi}_k^0,\tilde{l}_a}+C_{12}^{\tilde{\chi}_k^0,\tilde{l}_a}+C_{11}^{\tilde{\chi}_k^0,\tilde{l}_a}\right)\\ &+m_{\tilde{\chi}_k^0}g^{R*}_{l\tilde{\chi}_k^0\tilde{l}_a}g^L_{l\tilde{\chi}_k^0\tilde{l}_a}\left(C_0^{\tilde{\chi}_k^0,\tilde{l}_a}+C_1^{\tilde{\chi}_k^0,\tilde{l}_a}+C_2^{\tilde{\chi}_k^0,\tilde{l}_a}\right)\Bigg]. \end{aligned} \tag{41}$$

The left- and right-handed couplings of the charginos and the neutralinos are defined in the interaction Lagrangian,

$$\begin{aligned} &\bar{l}(ig^L_{l\tilde{\chi}_j^-\tilde{\nu}_i}P_L+ig^R_{l\tilde{\chi}_j^-\tilde{\nu}_i}P_R)\chi_j^-\tilde{\nu}_i\\ &+\bar{\chi}_k^0(ig^L_{l\tilde{\chi}_k^0\tilde{l}_a}P_L+ig^R_{l\tilde{\chi}_k^0\tilde{l}_a}P_R)l\tilde{l}_a^*, \end{aligned} \tag{42}$$

where

$$g^L_{l\tilde{\chi}_j^-\tilde{\nu}_i} = \frac{m_l}{vc_\beta}\left(U_{il}^{\tilde{\nu}}+iU_{i(l+9)}^{\tilde{\nu}}\right)U_{j2}^{\chi\,*}, \tag{43}$$

$$\begin{aligned} g^R_{l\tilde{\chi}_j^-\tilde{\nu}_i} = &-\frac{g_2V_{j1}^{\chi}}{\sqrt{2}}\left(U_{il}^{\tilde{\nu}}+iU_{i(l+9)}^{\tilde{\nu}}\right)\\ &+\frac{1}{\sqrt{2}}V_{j2}^{\chi}\left(U_{i(l+3)}^{\tilde{\nu}}+iU_{i(l+12)}^{\tilde{\nu}}\right)y_{ll}^{\nu*}, \end{aligned} \tag{44}$$

$$\begin{aligned} g^L_{l\tilde{\chi}_k^0\tilde{l}_a} = &\left(\frac{g_1}{\sqrt{2}}N_{k1}^*+\frac{g_2}{\sqrt{2}}N_{k2}^*\right)U_{a1}^{\tilde{l}}\\ &+\frac{\sqrt{2}m_l}{vc_\beta}N_{k3}^*U_{a2}^{\tilde{l}}, \end{aligned} \tag{45}$$

$$g^R_{l\tilde{\chi}_k^0\tilde{l}_a} = -\sqrt{2}g_1N_{k1}U_{a2}^{\tilde{l}}-\frac{\sqrt{2}m_l}{vc_\beta}N_{k3}U_{a1}^{\tilde{l}}, \tag{46}$$

where g_1 and g_2 are the gauge couplings of the $U(1)_Y$ and $SU(2)_L$ gauge groups, respectively. Note that we allow for lepton flavour mixing in the neutrino sector, therefore y^ν is a 3×3 complex matrix and y_{ll}^ν is the lth diagonal element with $l=1,2,3$ for electron, muon and tauon, respectively. For the complex NMSSM without inverse seesaw mechanism, one sets y^ν to zero and $U^\nu, U^{\tilde{\nu}}$ to a 3×3 unity matrix in the charged Higgs and chargino contributions. The neutralino contribution is the same in both models. In summary the new one-loop contributions from the weak sector of the NMSSM-nuSS to the leptonic AMM and EDM are given by

$$\begin{aligned} F_L^{\mathrm{new},1l} = &F_L^{\mathrm{new},W}+F_L^{\mathrm{new},H}+F_L^{\mathrm{NM},H^\pm}\\ &+F_L^{\mathrm{NM},\tilde{\chi}^\pm}+F_L^{\mathrm{NM},\tilde{\chi}^0}, \end{aligned} \tag{47}$$

$$a_l^{1l} = \mathrm{Re}[F_L^{\mathrm{new},1l}], \quad d_l^{1l} = \frac{e}{2m_l}\mathrm{Im}[F_L^{\mathrm{new},1l}]. \tag{48}$$

Finally, we define the abbreviations for the one-loop three-point integrals which have been used earlier in this section,

$$C^{x,y}_{i\ldots} = C_{i\ldots}\left(m_l^2, 0, m_l^2, m_x^2, m_y^2, m_y^2\right), \tag{49}$$

where the following conventions of the one-loop three-point integrals in $D = 4 - 2\epsilon$ are used

$$C_0^{x,y} = \frac{(\mu_R^2\pi)^{(4-D)/2}}{i\pi^2}\int d^Dq\frac{1}{D_{x,y}}, \tag{50}$$

$$C_1^{x,y}p_1^\mu + C_2^{x,y}p_2^\mu = \frac{(\mu_R^2\pi)^{(4-D)/2}}{i\pi^2}\int d^Dq\frac{q^\mu}{D_{x,y}}, \tag{51}$$

$$C_{00}^{x,y}g^{\mu\nu} + C_{11}^{x,y}p_1^\mu p_1^\nu + C_{12}^{x,y}(p_1^\mu p_2^\nu + p_1^\nu p_2^\mu) + C_{22}^{x,y}p_2^\mu p_2^\nu = \frac{(\mu_R^2\pi)^{(4-D)/2}}{i\pi^2}\int d^Dq\frac{q^\mu q^\nu}{D_{x,y}}, \tag{52}$$

where the denominator $D_{x,y}$ is given by

$$D_{x,y} = (q^2 - m_x^2)((q-p_1)^2 - m_y^2)((q-p_2)^2 - m_y^2), \tag{53}$$

with $p_1^2 = m_l^2$, $p_2^2 = m_l^2$, $(p_1 - p_2)^2 = 0$, m_l being the mass of the external lepton, $m_{x,y}$ being the masses of the particles x and y. If $m_l \ll m_x, m_y$ one can use the zero external mass approximation for these coefficients [44],

$$C_0(0,0,0,x,y,y) = \frac{1}{x}\left(-\frac{1}{t-1} + \frac{\ln(t)}{(t-1)^2}\right), \tag{54}$$

$$C_1(0,0,0,x,y,y) = \frac{1}{x}\left(\frac{(t-3)}{4(t-1)^2} + \frac{\ln(t)}{2(t-1)^3}\right), \tag{55}$$

$$C_{11}(0,0,0,x,y,y) = \frac{1}{x}\left(\frac{(-2t^2+7t-11)}{18(t-1)^3} + \frac{\ln(t)}{3(t-1)^4}\right), \tag{56}$$

$$C_2(0,0,0,x,y,y) = C_1(0,0,0,x,y,y), \tag{57}$$

$$C_{22}(0,0,0,x,y,y) = 2C_{12}(0,0,0,x,y,y) = C_{11}(0,0,0,x,y,y), \tag{58}$$

where $t = y/x$. If m_l is of the order of the internal masses, one should use the following expressions

$$C_0(m,0,m,x,y,y) = \int_0^1 \frac{zdz}{-mz^2 + (m+x-y)z - x}, \tag{59}$$

$$C_1(m,0,m,x,y,y) = \int_0^1 \frac{-z^2dz}{2(-mz^2 + (m+x-y)z - x)}, \tag{60}$$

$$C_{11}(m,0,m,x,y,y) = \int_0^1 \frac{z^3dz}{3(-mz^2 + (m+x-y)z - x)}, \tag{61}$$

$$C_2(m,0,m,x,y,y) = C_1(m,0,m,x,y,y), \tag{62}$$

$$C_{22}(m,0,m,x,y,y) = 2C_{12}(m,0,m,x,y,y) = C_{11}(m,0,m,x,y,y). \tag{63}$$

We have implemented the analytic expressions of these one-loop three-point integral coefficients including the dependence on m_l^2 and compared with the numerical results obtained from the Package-X [45]. The zero external mass approximation can be applied for chargino and neutralino one-loop diagrams, and we then recover the known formula in the MSSM [46]. To the best of our knowledge, this is the first time that the full one-loop SUSY corrections to the leptonic AMM and EDM in the complex NMSSM with inverse seesaw mechanism have been presented. For the NMSSM without inverse seesaw mechanism, the expressions of the full one-loop contributions to the muon AMM have been presented in [24] and the full one-loop contributions to the electron EDM have been discussed in [47]. The one-loop chargino and neutralino contributions are always considered to be dominant in most of the parameter space, so that they are the only ones taken into account in the analyses of the muon and electron AMM available in the literature [34,35]. However in case of light sterile neutrino masses and/or light singlet-like Higgs bosons, contributions from W and/or Higgs diagrams can be significant. Therefore, for the investigation of the full parameter space these contributions should be taken into account.

3.2 Two-loop contributions

The two-loop SUSY contributions to the muon AMM in the MSSM have been classified and evaluated in [48–54] for the CP-conserving case and in [55] for the CP-violating case. The numerical results of all two-loop contributions have identified some dominant contributions. These dominant two-loop SUSY corrections have been generalized to the CP-conserving NMSSM and implemented in `NMSSMTools` [24]. We follow this strategy to take into account the dominant two-loop contributions. We first consider the leading-logarithmic two-loop electroweak contribution which arises from the SUSY one-loop diagrams with an additional photon loop. This contribution has been evaluated most efficiently by using the effective Lagrangian approach which can be applied for the SM and many new physic models, as performed in [56]. It is given by

$$a_l^{\text{qed},2l} = -\frac{4\alpha}{\pi}a_l^{\text{new},1l}\log\frac{M_{\text{SUSY}}}{m_l},$$
$$d_l^{\text{qed},2l} = -\frac{4\alpha}{\pi}d_l^{\text{new},1l}\log\frac{M_{\text{SUSY}}}{m_l}, \tag{64}$$

where the scale M_{SUSY} is chosen to be of the order of the masses of the smuons, in particular $M_{\text{SUSY}} = \sqrt{m_{\tilde{\mu}_R}m_{\tilde{\mu}_L}}$. The negative sign of this term gives a reduction of about ten percent of the whole one-loop contribution.

The Higgs-mediated Barr–Zee-type diagrams [57] with an internal photon can contribute significantly to the leptonic AMM. We consider here the contributions from fermion loops, sfermion loops, charged Higgs loops and chargino loops generating the effective $h_i\gamma\gamma$ vertex. These contributions can be calculated by evaluating first the effective $h_i\gamma\gamma$ vertex and then inserting this effective vertex into the second loop. Making use of gauge invariance, the effective $h_i\gamma\gamma$ vertex can be written as[1]

$$\Gamma^{\mu\nu}_{h_i\gamma\gamma^*} = ((k\cdot q)g^{\mu\nu} - q^\mu k^\nu)\Gamma^A + \epsilon^{\mu\nu\alpha\beta}k_\alpha q_\beta \Gamma^P, \quad (65)$$

where k^μ, q^ν are the momenta of the on-shell and off-shell photons, respectively, and Γ^A, Γ^P are scalar form factors. We evaluate these form factors for sfermion loops, charged Higgs loops, chargino loops and fermion loops. They are given by

$$\Gamma^A_{\tilde f} = -\frac{N_c^f Q_{\tilde f}^2 e^2 g_{h_i\tilde f^*\tilde f} v}{8\pi^2}\int_0^1 dx \frac{x(x-1)}{q^2x(1-x)-M^2_{\tilde f}}, \quad (66)$$

$$\Gamma^P_{\tilde f} = 0, \quad (67)$$

$$\Gamma^A_{H^\pm} = -\frac{e^2 g_{h_i H^+H^-} v}{8\pi^2}\int_0^1 dx \frac{x(x-1)}{q^2x(1-x)-M^2_{H^\pm}}, \quad (68)$$

$$\Gamma^P_{H^\pm} = 0, \quad (69)$$

$$\Gamma^A_{\tilde\chi^\pm} = \frac{e^3 g^S_{h_i\tilde\chi_j^+\tilde\chi_j^-} M_{\tilde\chi_j^\pm}}{4\pi^2\sqrt{2}s_W}\int_0^1 dx \frac{2x(x-1)+1}{q^2x(1-x)-M^2_{\tilde\chi_j^\pm}}, \quad (70)$$

$$\Gamma^P_{\tilde\chi^\pm} = \frac{e^3 g^P_{h_i\tilde\chi_j^+\tilde\chi_j^-} M_{\tilde\chi_j^\pm}}{4\pi^2\sqrt{2}s_W}\int_0^1 dx \frac{1}{q^2x(1-x)-M^2_{\tilde\chi_j^\pm}}, \quad (71)$$

$$\Gamma^A_f = \frac{N_c^f Q_f^2 e^2 g^S_{h_i\bar f f} m_f^2}{4\pi^2 v}\int_0^1 dx \frac{2x(x-1)+1}{q^2x(1-x)-m_f^2}, \quad (72)$$

$$\Gamma^P_f = \frac{N_c^f Q_f^2 e^2 g^P_{h_i\bar f f} m_f^2}{4\pi^2 v}\int_0^1 dx \frac{1}{q^2x(1-x)-m_f^2}, \quad (73)$$

where $Q_{f/\tilde f}$ is the electric charge of fermion f/of sfermion $\tilde f$, $N_c = 3$ for quarks and $N_c = 1$ for leptons. We take into account only the third generation of quarks and leptons in the loops since they have significant Yukawa couplings. We used the following convention for the couplings of the neutral Higgs boson h_i to fermions, sfermions, charged Higgs bosons and charginos,

$$\begin{aligned}
&-\frac{im_f}{v}\bar f(g^S_{h_i\bar f f} + ig^P_{h_i\bar f f}\gamma_5) f h_i \\
&-\frac{ig_2}{\sqrt{2}}\bar\chi_j^-(g^S_{h_i\tilde\chi_j^+\tilde\chi_j^-} + ig^P_{h_i\tilde\chi_j^+\tilde\chi_j^-}\gamma_5)\chi_j^- h_i \\
&+ iv g_{h_i H^+H^-} h_i H^+H^- + iv g_{h_i\tilde f_k^*\tilde f_k} h_i \tilde f_k^*\tilde f_k, \quad (74)
\end{aligned}$$

with the explicit expressions for $g^{S/P}_{h_i\bar f f}$, $g^{S/P}_{h_i\tilde\chi_j^+\tilde\chi_j^-}$, $g_{h_iH^+H^-}$, and $g_{h_i\tilde f_k^*\tilde f_k}$ given by

$$g^S_{h_i\bar f f} = \frac{\mathcal{R}^H_{i1}}{c_\beta}, \quad g^P_{h_i\bar f f} = -\mathcal{R}^H_{i4}t_\beta, \quad f = b,\tau,e,\mu, \quad (75)$$

$$g^S_{h_i\bar f f} = \frac{\mathcal{R}^H_{i2}}{s_\beta}, g^P_{h_i\bar f f} = -\frac{\mathcal{R}^H_{i4}}{t_\beta}, \quad f = t, \quad (76)$$

$$\begin{aligned}
g^S_{h_i\tilde\chi_j^+\tilde\chi_j^-} = \mathrm{Re}\Big[&U^\chi_{j2}V^\chi_{j1}\mathcal{R}^H_{i1} + e^{i\varphi_u}U^\chi_{j1}V^\chi_{j2}\mathcal{R}^H_{i2} \\
&+ e^{-i\varphi_s}\frac{\lambda^*}{g_2}U^\chi_{j2}V^\chi_{j2}\mathcal{R}^H_{i3}\Big] \\
&- \mathrm{Im}[s_\beta U^\chi_{j2}V^\chi_{j1} + e^{i\varphi_u}c_\beta U^\chi_{j1}V^\chi_{j2}]\mathcal{R}^H_{i4} \\
&+ \mathrm{Im}\Big[\frac{\lambda^* e^{-i\varphi_s}}{g_2}U_{j2}V_{j2}\Big]\mathcal{R}^H_{i5}, \quad (77)
\end{aligned}$$

$$\begin{aligned}
g^P_{h_i\tilde\chi_j^+\tilde\chi_j^-} = \mathrm{Im}\Big[&U^\chi_{j2}V^\chi_{j1}\mathcal{R}^H_{i1} + e^{i\varphi_u}U^\chi_{j1}V^\chi_{j2}\mathcal{R}^H_{i2} \\
&+ e^{-i\varphi_s}\frac{\lambda^*}{g_2}U^\chi_{j2}V^\chi_{j2}\mathcal{R}^H_{i3}\Big] \\
&+ \mathrm{Re}[s_\beta U^\chi_{j2}V^\chi_{j1} + e^{i\varphi_u}c_\beta U^\chi_{j1}V^\chi_{j2}]\mathcal{R}^H_{i4} \\
&- \mathrm{Re}\Big[\frac{\lambda^* e^{-i\varphi_s}}{g_2}U^\chi_{j2}V^\chi_{j2}\Big]\mathcal{R}^H_{i5}, \quad (78)
\end{aligned}$$

$$\begin{aligned}
g_{h_iH^+H^-} = &\left(\frac{g_1^2c_\beta c_{2\beta}}{4} - \frac{g_2^2c_\beta(1+2s_\beta^2)}{4} + c_\beta s_\beta^2|\lambda|^2\right)\mathcal{R}^H_{i1} \\
&+\left(-\frac{g_1^2 s_\beta c_{2\beta}}{4} - \frac{g_2^2 s_\beta(1+2c_\beta^2)}{4} + c_\beta^2 s_\beta|\lambda|^2\right)\mathcal{R}^H_{i2} \\
&+\Big(-\frac{s_{2\beta}\mathrm{Re}[A_\lambda\lambda e^{i(\varphi_u+\varphi_s)}]}{\sqrt{2}v} \\
&-\frac{s_{2\beta}v_s\mathrm{Re}[\kappa^*\lambda e^{i(\varphi_u-\varphi_s)}]}{v} - \frac{|\lambda|^2 v_s}{v}\Big)\mathcal{R}^H_{i3} \\
&+\Big(\frac{s_{2\beta}\mathrm{Im}[A_\lambda\lambda e^{i(\varphi_u+\varphi_s)}]}{\sqrt{2}v} \\
&-\frac{s_{2\beta}v_s\mathrm{Im}[\kappa^*\lambda e^{i(\varphi_u-\varphi_s)}]}{v}\Big)\mathcal{R}^H_{i5}, \quad (79)
\end{aligned}$$

$$\begin{aligned}
g_{h_i\tilde f_k^*\tilde f_k} = &\left(\frac{g_1^2}{12}c_\beta(|U^{\tilde f}_{k1}|^2 - 4|U^{\tilde f}_{k2}|^2) - \frac{g_2^2}{4}c_\beta|U^{\tilde f}_{k1}|^2\right. \\
&\left.+\frac{y_t v_s\mathrm{Re}[\lambda e^{I\varphi_s}U^{\tilde f *}_{k1}U^{\tilde f}_{k2}]}{v}\right)\mathcal{R}^H_{i1} \\
&+\Big(\frac{g_1^2}{12}s_\beta(-|U^{\tilde f}_{k1}|^2 + 4|U^{\tilde f}_{k2}|^2) \\
&+\frac{g_2^2}{4}s_\beta|U^{\tilde f}_{k1}|^2 + y_t^2 s_\beta(|U^{\tilde f}_{k1}|^2 + |U^{\tilde f}_{k2}|^2)
\end{aligned}$$

[1] In the actual calculation, there may appear some gauge-dependent terms proportional to $q^\mu q^\nu$ and to $g^{\mu\nu}$. They do not contribute, however, to the EDM and the AMM at two-loop level as shown in [58,59].

$$
\begin{aligned}
&- \frac{\sqrt{2} y_t \mathrm{Re}[A_t e^{i\varphi_u} U^{\tilde{t}*}_{k1} U^{\tilde{t}}_{k2}]}{v}\Big)\mathcal{R}^H_{i2} \\
&+ \mathrm{Re}[\lambda e^{i\varphi_s} U^{\tilde{t}}_{k1} U^{\tilde{t}*}_{k2}] y_t c_\beta \mathcal{R}^H_{i3} \\
&+ \Bigg(-\frac{\mathrm{Im}[\lambda e^{i\varphi_s} U^{\tilde{t}}_{k1} U^{\tilde{t}*}_{k2}] y_t v_s s_\beta}{v} \\
&+ \frac{\sqrt{2} c_\beta y_t \mathrm{Im}[A_f e^{i\varphi_u} U^{\tilde{t}*}_{k1} U^{\tilde{t}}_{k2}]}{v}\Bigg)\mathcal{R}^H_{i4} \\
&- c_\beta y_t \mathrm{Im}[\lambda e^{i\varphi_s} U^{\tilde{t}}_{k1} U^{\tilde{t}*}_{k2}]\mathcal{R}^H_{i5}, \qquad (80)
\end{aligned}
$$

$$
\begin{aligned}
g_{h_i \tilde{b}^*_k \tilde{b}_k} = &\Big(\frac{g_1^2}{12} c_\beta (|U^{\tilde{b}}_{k1}|^2 + 4|U^{\tilde{b}}_{k2}|^2) \\
&+ \frac{g_2^2}{4} c_\beta |U^{\tilde{b}}_{k1}|^2 - y_b^2 c_\beta (U^{\tilde{b}*}_{k1} U^{\tilde{b}}_{k1} + U^{\tilde{b}*}_{k2} U^{\tilde{b}}_{k2}) \\
&- \frac{\sqrt{2} y_b \mathrm{Re}[A_b U^{\tilde{b}*}_{k1} U^{\tilde{b}}_{k2}]}{v}\Big)\mathcal{R}^H_{i1} \\
&+ \Big(\frac{g_1^2}{12} s_\beta (-|U^{\tilde{b}}_{k1}|^2 - 2|U^{\tilde{b}}_{k2}|^2) \\
&- \frac{g_2^2}{4} s_\beta |U^{\tilde{t}}_{k1}|^2 + \frac{y_b v_s \mathrm{Re}[\lambda e^{i(\varphi_u+\varphi_s)} U^{\tilde{b}}_{k1} U^{\tilde{b}*}_{k2}]}{v}\Big)\mathcal{R}^H_{i2} \\
&+ \mathrm{Re}[\lambda e^{i(\varphi_s+\varphi_u)} U^{\tilde{b}}_{k1} U^{\tilde{b}*}_{k2}] y_b s_\beta \mathcal{R}^H_{i3} \\
&+ \Bigg(-\frac{\mathrm{Im}[\lambda e^{i(\varphi_s+\varphi_u)} U^{\tilde{b}}_{k1} U^{\tilde{b}*}_{k2}] y_t v_s c_\beta}{v} \\
&+ \frac{\sqrt{2} s_\beta y_b \mathrm{Im}[A_b U^{\tilde{b}*}_{k1} U^{\tilde{b}}_{k2}]}{v}\Bigg)\mathcal{R}^H_{i4} \\
&- s_\beta y_b \mathrm{Im}[\lambda e^{i(\varphi_s+\varphi_u)} U^{\tilde{b}}_{k1} U^{\tilde{b}*}_{k2}]\mathcal{R}^H_{i5}, \qquad (81)
\end{aligned}
$$

$$
\begin{aligned}
g_{h_i \tilde{\tau}^*_k \tilde{\tau}_k} = &\Big(\frac{g_1^2}{4} c_\beta (|U^{\tilde{\tau}}_{k1}|^2 - 2|U^{\tilde{\tau}}_{k2}|^2) \\
&+ \frac{g_2^2}{4} c_\beta |U^{\tilde{\tau}}_{k1}|^2 - y_\tau^2 c_\beta (U^{\tilde{\tau}*}_{k1} U^{\tilde{\tau}}_{k1} + U^{\tilde{\tau}*}_{k2} U^{\tilde{\tau}}_{k2}) \\
&- \frac{\sqrt{2} y_\tau \mathrm{Re}[A_\tau U^{\tilde{\tau}*}_{k1} U^{\tilde{\tau}}_{k2}]}{v}\Big)\mathcal{R}^H_{i1} \\
&+ \Big(\frac{g_1^2}{4} s_\beta (|U^{\tilde{\tau}}_{k1}|^2 - 2|U^{\tilde{\tau}}_{k2}|^2) \\
&- \frac{g_2^2}{4} s_\beta |U^{\tilde{\tau}}_{k1}|^2 + \frac{y_\tau v_s \mathrm{Re}[\lambda e^{i(\varphi_u+\varphi_s)} U^{\tilde{\tau}}_{k1} U^{\tilde{\tau}*}_{k2}]}{v}\Big)\mathcal{R}^H_{i2} \\
&+ \Bigg(-\frac{\mathrm{Im}[\lambda e^{i(\varphi_s+\varphi_u)} U^{\tilde{\tau}}_{k1} U^{\tilde{\tau}*}_{k2}] y_\tau v_s c_\beta}{v} \\
&+ \frac{\sqrt{2} s_\beta y_\tau \mathrm{Im}[A_\tau U^{\tilde{\tau}*}_{k1} U^{\tilde{\tau}}_{k2}]}{v}\Bigg)\mathcal{R}^H_{i4} \\
&+ \mathrm{Re}[\lambda e^{i(\varphi_s+\varphi_u)} U^{\tilde{\tau}}_{k1} U^{\tilde{\tau}*}_{k2}] y_\tau s_\beta \mathcal{R}^H_{i3} \\
&- s_\beta y_\tau \mathrm{Im}[\lambda e^{i(\varphi_s+\varphi_u)} U^{\tilde{\tau}}_{k1} U^{\tilde{\tau}*}_{k2}]\mathcal{R}^H_{i5}. \qquad (82)
\end{aligned}
$$

The gauge invariant form of the effective $h_i\gamma\gamma$ coupling in (65) will be inserted into the second loop to get the AMM and EDM. The lepton mass in the numerator of the second loop is neglected, since this leads to contributions suppressed by the factor m_l^2/M_S^2 where M_S is the mass of the heavy particles. We present here the analytic expressions for the AMM from sfermion loops, charged Higgs loops, chargino loops and fermion loops,

$$
a_l^{\tilde{f},2l} = \sum_{i=1}^{5} \frac{N_c^f Q_{\tilde{f}}^2 \alpha m_l^2}{16\pi^3 m_{h_i}^2} (g^S_{h_i \bar{l} l} g_{h_i \tilde{f}^* \tilde{f}}) \mathcal{F}^{(2)}\left(\frac{M^2_{\tilde{f}}}{m^2_{h_i}}\right), \qquad (83)
$$

$$
a_l^{H^\pm,2l} = \sum_{i=1}^{5} \frac{\alpha m_l^2}{16\pi^3 m_{h_i}^2} (g^S_{h_i \bar{l} l} g_{h_i H^+ H^-}) \mathcal{F}^{(2)}\left(\frac{M^2_{H^\pm}}{m^2_{h_i}}\right), \qquad (84)
$$

$$
\begin{aligned}
a_l^{\tilde{\chi}^\pm,2l} = &\sum_{i=1}^{5}\sum_{j=1}^{2} \frac{\alpha^2 m_l^2}{2\sqrt{2}\pi^2 M_W s_W^2} \frac{1}{M_{\tilde{\chi}^\pm_j}} \\
&\times \Bigg(g^S_{h_i \bar{l} l} g^S_{h_i \tilde{\chi}^+_j \tilde{\chi}^-_j} \mathcal{F}^{(1)}\left(\frac{M^2_{\tilde{\chi}^\pm_j}}{m^2_{h_i}}\right) \\
&- g^P_{h_i \bar{l} l} g^P_{h_i \tilde{\chi}^+_j \tilde{\chi}^-_j} \mathcal{G}\left(\frac{M^2_{\tilde{\chi}^\pm_j}}{m^2_{h_i}}\right)\Bigg), \qquad (85)
\end{aligned}
$$

$$
\begin{aligned}
a_l^{f,2l} = &\sum_{i=1}^{5} \frac{N_c^f Q_f^2 \alpha^2 m_l^2}{4\pi^2 M_W^2 s_W^2} \\
&\times \Bigg(g^S_{h_i \bar{l} l} g^S_{h_i \bar{f} f} \mathcal{F}^{(1)}\left(\frac{m_f^2}{m^2_{h_i}}\right) \\
&- g^P_{h_i \bar{l} l} g^P_{h_i \bar{f} f} \mathcal{G}\left(\frac{m_f^2}{m^2_{h_i}}\right)\Bigg), \qquad (86)
\end{aligned}
$$

where α is the fine structure constant and the two-loop functions are given by

$$
\mathcal{F}^{(2)}(z) = \int_0^1 dx \frac{x(1-x)}{z + x(x-1)} \ln \frac{x(1-x)}{z}, \qquad (87)
$$

$$
\mathcal{F}^{(1)}(z) = \frac{z}{2} \int_0^1 dx \frac{1 - 2x(1-x)}{x(1-x) - z} \ln \frac{x(1-x)}{z}, \qquad (88)
$$

$$
\mathcal{G}(z) = \frac{z}{2} \int_0^1 dx \frac{1}{x(1-x) - z} \ln \frac{x(1-x)}{z}. \qquad (89)
$$

Note that these expressions are in agreement with Eq. (3.8) of Ref. [55] for the complex MSSM, we used, however, a different sign convention compared to their notation. These two-loop contributions are then subtracted from the corresponding SM contributions arising from top, bottom quark and tau lepton loops. The leptonic EDM can be obtained from the above formulae with the replacement

$$
\begin{aligned}
&d_l^{x,2l} = \frac{e}{2m_l} a_l^{x,2l} (g^S_{h_i \bar{l} l} \to g^P_{h_i \bar{l} l}, g^P_{h_i \bar{l} l} \to -g^S_{h_i \bar{l} l}), \\
&x = \tilde{f}, H^\pm, \tilde{\chi}^\pm, f. \qquad (90)
\end{aligned}
$$

The two-loop Barr–Zee-type contributions[2] to the electron EDM have been implemented in NMSSMCALC as described in Ref. [47]. It does not only contain contributions coming from the effective $h_i\gamma\gamma$ vertex but also other contributions arising from the effective $h_i\gamma Z$, $H^\pm\gamma W^\mp$, $H^\pm\gamma W^\mp$ vertices. Since there is no difference between the two models in these contributions we keep them unchanged in NMSSMCAL-nuSS.

In summary, the SUSY contributions to the leptonic AMM and EDM considered in this study are the sum of the full one-loop and partial two-loop contributions,

$$\begin{aligned} a_l &= a_l^{1l} + a_l^{\text{qed},2l} + a_l^{\tilde{f},2l} + a_l^{H^\pm,2l} + a_l^{\tilde{\chi}^\pm,2l} \\ &\quad + (a_l^{f,2l} - a_l^{\text{SM},f,2l}) \end{aligned} \tag{91}$$

$$\begin{aligned} d_l &= d_l^{1l} + d_l^{\text{qed},2l} + d_l^{\tilde{f},2l} + d_l^{H^\pm,2l} + d_l^{\tilde{\chi}^\pm,2l} \\ &\quad + (a_l^{f,2l} - a_l^{\text{SM},f,2l}) + d_l^{2l}(h_i\gamma Z) + d_l^{2l}(H^\pm\gamma W^\mp) \\ &\quad + d_l^{2l}(H^\pm\gamma W^\mp) \end{aligned} \tag{92}$$

where $d_l^{2l}(h_i\gamma Z) + d_l^{2l}(H^\pm\gamma W^\mp) + d_l^{2l}(H^\pm\gamma W^\mp)$ are the two-loop Barr–Zee-type contributions arising from the effective $h_i\gamma Z$, $H^\pm\gamma W^\mp$, $H^\pm\gamma W^\mp$ vertices.

4 Numerical analysis

In this section we investigate the numerical impact of the neutrino/sneutrino sector and various CP-violating phases on the muon AMM and on the electron EDM. It has been shown in our study in [31], that the extended neutrino and sneutrino sectors can have a significant impact on the Higgs sector, the charged lepton flavor-violating decays, $l_i \to l_j + \gamma$, and the new physics constraints from the oblique parameters S, T, U. We therefore will investigate also what is the correlation between these impacts. In order to find viable parameter points we performed a scan in the NMSSM parameter space. We have used NMSSMCALC-nuSS to calculate the Higgs boson masses including the available two-loop corrections at $\mathcal{O}(\alpha_s\alpha_t + \alpha_t^2)$,[3] the Higgs decay widths and branching ratios including the state-of-the-art higher-order QCD corrections as well as the Higgs effective couplings. We then use HiggsBounds [61] to check if the parameter points pass all the exclusion limits from the searches at LEP, Tevatron and the LHC, and HiggsSignals-2.6.1 [62] to check if the points are consistent with the LHC data for a 125 GeV Higgs boson. A parameter point is chosen if it is consistent with the Higgs data within 2σ. With our NMSSMCALC-nuSS code we can also check if the parameter point is in accordance with the active light neutrino data,[4] the constraints from the charged lepton flavor-violating decays and the electroweak observables, see [31] for more information.

In order to show the impact of the neutrino Yukawa couplings on the AMM we choose a sample parameter point from our generated scan sample satisfying all the mentioned constraints, called P1 in the following. The SM input parameters are taken from the Particle Data Group [63] and are given by

$$\begin{aligned} \alpha(M_Z) &= 1/127.955, & \alpha_s^{\overline{\text{MS}}}(M_Z) &= 0.1181, \\ M_Z &= 91.1876\ \text{GeV}, & M_W &= 80.379\ \text{GeV}, \\ m_t &= 172.74\ \text{GeV}, & m_b^{\overline{\text{MS}}}(m_b^{\overline{\text{MS}}}) &= 4.18\ \text{GeV}, \\ m_c &= 1.274\ \text{GeV}, & m_s &= 95.0\ \text{MeV}, \\ m_u &= 2.2\ \text{MeV}, & m_d &= 4.7\ \text{MeV}, \\ m_\tau &= 1.77682\ \text{GeV}, & m_\mu &= 105.6584\ \text{MeV}, \\ m_e &= 510.9989\ \text{keV}, & G_F &= 1.16637 \cdot 10^{-5}\ \text{GeV}^{-2}. \end{aligned} \tag{93}$$

The light neutrino input parameters are set equal to their best-fit values [63] together with a fixed value for the lightest neutrino mass, in particular,

$$\begin{aligned} m_{\nu_1} &= 10^{-11}\ \text{GeV}, & \theta_{12} &= \arcsin(\sqrt{0.297}), \\ m_{\nu_2} &= \sqrt{m_{\nu_1}^2 + 7.37 \times 10^{-23}}\ \text{GeV}, & \theta_{23} &= \arcsin(\sqrt{0.425}), \\ m_{\nu_3} &= \sqrt{m_{\nu_1}^2 + 2.525 \times 10^{-21}}\ \text{GeV}, & \theta_{13} &= \arcsin(\sqrt{0.0215}), \\ & & \delta_{CP} &= 248.4^\circ. \end{aligned}$$

All other complex phases are set to zero and the remaining input parameters are given by

$$\begin{aligned} M_{H^\pm} &= 1000\ \text{GeV}, & m_{\tilde{\mu}_L} &= 400\ \text{GeV}, \\ M_1 &= 400\ \text{GeV}, & m_{\tilde{\mu}_R} &= m_{\tilde{q}_L} = m_{\tilde{q}_R} = 2000\ \text{GeV}, \\ M_2 &= 400\ \text{GeV}, & m_{\tilde{X}} &= 0\ \text{GeV}, \\ \mu_{\text{eff}} &= 400\ \text{GeV}, & m_{\tilde{N}} &= 0\ \text{GeV}, \\ m_{\tilde{Q}_3} &= 1000\ \text{GeV}, & A_{11}^\nu = A_{33}^\nu &= 1000\ \text{GeV}, \\ m_{\tilde{t}_R} &= 1500\ \text{GeV}, & A_{22}^\nu &= -1000\ \text{GeV}, \\ m_{\tilde{e}_L} = m_{\tilde{\tau}_L} &= 2000\ \text{GeV}, & A_X &= 1000\ \text{GeV}, \\ m_{\tilde{e}_R} = m_{\tilde{\tau}_R} &= 2000\ \text{GeV}, & \mu_X &= 600\ \text{GeV}, \\ A_t &= 2000\ \text{GeV}, & B_{\mu_X} &= 10\ \text{GeV}, \\ \text{Re}A_k &= -100\ \text{GeV}, & y_{11}^\nu = y_{33}^\nu &= 0.5, \quad i = 1,2,3, \\ \tan\beta &= 12, & y_{22}^\nu &= 0.9, \\ \lambda &= 0.252, & \kappa &= 0.297. \end{aligned} \tag{94}$$

Note that we have used the μ_X-parameterization where the neutrino Yukawa couplings y^ν are given as inputs. For the parameter point P1, we have chosen y^ν to be a diagonal matrix. With this choice, we do not need to worry about the violation of the charged lepton flavor-violating decays, $l_i \to$

[2] The contribution from the two-loop rainbow-like diagrams can be compatible to the Barr–Zee-type contribution in the very large sfermion mass region [60].

[3] Note that we have taken into account the complete one-loop corrections computed in the NMSSM with inverse seesaw mechanism [31], but took over the two-loop corrections from the pure NMSSM.

[4] The non-unitary constraint on the first 3×3 block of the neutrino rotation matrix U^ν is included also in the active light neutrino data. The implementation of this constraint has been described in [31].

Table 1 Parameter point P1: Mass values in GeV and main components of the neutral Higgs bosons at two-loop $\mathcal{O}(\alpha_t\alpha_s+\alpha_t^2)$ obtained for the NMSSM without and with the inverse seesaw mechanism using OS renormalization in the top/stop sector

		h_1	h_2	h_3	h_4	h_5
$\mathcal{O}(\alpha_t\alpha_s+\alpha_t^2)$	Without ISS	124.2	369.59	912.37	998.91	999.94
	With ISS	125.46	369.65	912.40	998.85	1000.0
Main component		h_u	a_s	h_d	a	h_s

Table 2 Electroweakino and smuon masses in GeV for the parameter point P1

$\tilde{\chi}_1^0$	$\tilde{\chi}_2^0$	$\tilde{\chi}_3^0$	$\tilde{\chi}_4^0$	$\tilde{\chi}_5^0$	$\tilde{\chi}_1^+$	$\tilde{\chi}_2^+$	$\tilde{\mu}_1$	$\tilde{\mu}_2$
331.93	400.00	405.14	470.96	945.1	341.19	461.72	402.83	2000

Table 3 The individual contributions to the muon AMM in the NMSSM without inverse seesaw mechanism. The total sum is given in the last column. All values are normalized to 10^{-10}

$a_\mu^{\tilde{\chi}^0,1l}$	$a_\mu^{\tilde{\chi}^\pm,1l}$	$a_\mu^{H,1l}$	$a_\mu^{H^\pm,1l}$	$a_\mu^{\text{qed},2l}$	$a_\mu^{\tilde{f},2l}$	$a_\mu^{f,2l}$	$a_\mu^{H^\pm,2l}$	$a_\mu^{\tilde{\chi}^\pm,2l}$	a_μ
-1.30	11.55	2×10^{-5}	-6×10^{-6}	-2.90	3×10^{-3}	-3×10^{-2}	3×10^{-4}	-6×10^{-2}	7.26

$l_j+\gamma$. In Table 1, we present the Higgs mass spectrum with and without inverse seesaw mechanism at two-loop $\mathcal{O}(\alpha_t\alpha_s+\alpha_t^2)$ using the OS renormalization for the top/stop sector. For the parameter point P1, the stop masses in the OS scheme are given by

$$m_{\tilde{t}_1}=1001.62\ \text{GeV},\quad m_{\tilde{t}_2}=1524.9\ \text{GeV}. \tag{95}$$

The main components of the Higgs mass eigenstates are also shown in the last row.

As can be inferred from Table 1, the neutrino/sneutrino sector increases the loop correction to the SM-like Higgs boson given by the h_u-like state. The spectrum[5] of the electroweakinos and smuons is the same in both models and is given in Table 2.

In the sneutrino sector, the left-handed muon dominated sneutrino mass is about 394.84 GeV in the NMSSM without inverse seesaw mechanism. In the NMSSM-nuSS, the muon-type sneutrino is the lightest superparticle (LSP) and has a mass of 261.6 GeV. While the pure left-handed sneutrino in the MSSM is excluded as the LSP and as a dark matter candidate [64], here, the lightest particles are not purely left-handed. There is a significant admixture of the left-handed muon-type, N-type and X-type sneutrinos. A careful study is needed to justify if these particles are good LSPs. We leave this point for a future study. In the NMSSM without inverse seesaw mechanism the LSP is given by the wino-like neutralino.

Impact on the muon AMM: In Table 3 we present for the NMSSM without inverse seesaw mechanism the individual contributions to the muon AMM as well as its total value. If not stated otherwise the results of the AMM of the muon are normalized to 10^{-10}. The dominant contribution comes from the chargino one-loop diagram. The contributions from the neutral Higgs and charged Higgs one-loop diagrams are very small since they are both proportional to m_μ^4. The second and third important contributions are the two-loop SUSY QED and the neutralino one-loop ones. They are both negative. The other two-loop contributions are small and negligible for the parameter point P1 where the masses of the non-SM-like Higgs bosons and the SUSY particles are rather heavy.

In the NMSSM-nuSS, the neutrino/sneutrino sector significantly changes the one-loop and the two-loop QED contributions while the two-loop contributions including the $h_i\gamma\gamma$ effective couplings remain unchanged w.r.t. the pure NMSSM. We present in Table 4 the individual contributions from the one-loop diagrams as well as the two-loop QED contribution to the AMM of the muon and its total sum. With the light sneutrino masses and large muon-neutrino Yukawa coupling y_{22}^ν, the chargino one-loop contribution has increased by a factor of about 2.3 compared to that of the NMMSM without ISS. The same behavior has been observed in Ref. [34]. This can be seen explicitly from the coupling $g^R_{l\tilde{\chi}_j^-\tilde{\nu}_i}$ of the chargino with the muon and the sneutrino presented in (44) where the second term is proportional to the neutrino Yukawa coupling y_{ll}^ν. Depending on the relative sign between the first and the second term in $g^R_{l^+\tilde{\chi}_j^-\tilde{\nu}_i}$, as well as on the sneutrino spectrum, the sneutrino contribution can increase or decrease the one-loop chargino contribution. A surprisingly large change is also observed in the W-boson and charged Higgs one-loop contributions. Note that we sub-

[5] The masses of neutralinos, charginos and left-handed smuon satisfy constraints for electroweakinos at the LHC.

Table 4 The individual one-loop and two-loop QED contributions to the AMM of the muon in the NMSSM-nuSS. The sum of all contributions is presented in the last column. All values are normalized to 10^{-10}

$a_\mu^{\tilde{\chi}^0,1l}$	$a_\mu^{\tilde{\chi}^\pm,1l}$	$a_\mu^{H,1l}$	$a_\mu^{H^\pm,1l}$	$a_\mu^{W,1l}$	$a_\mu^{\text{qed},2l}$	a_μ
−1.3	26.99	2×10^{-5}	−0.286	−1.3	−6.82	17.21

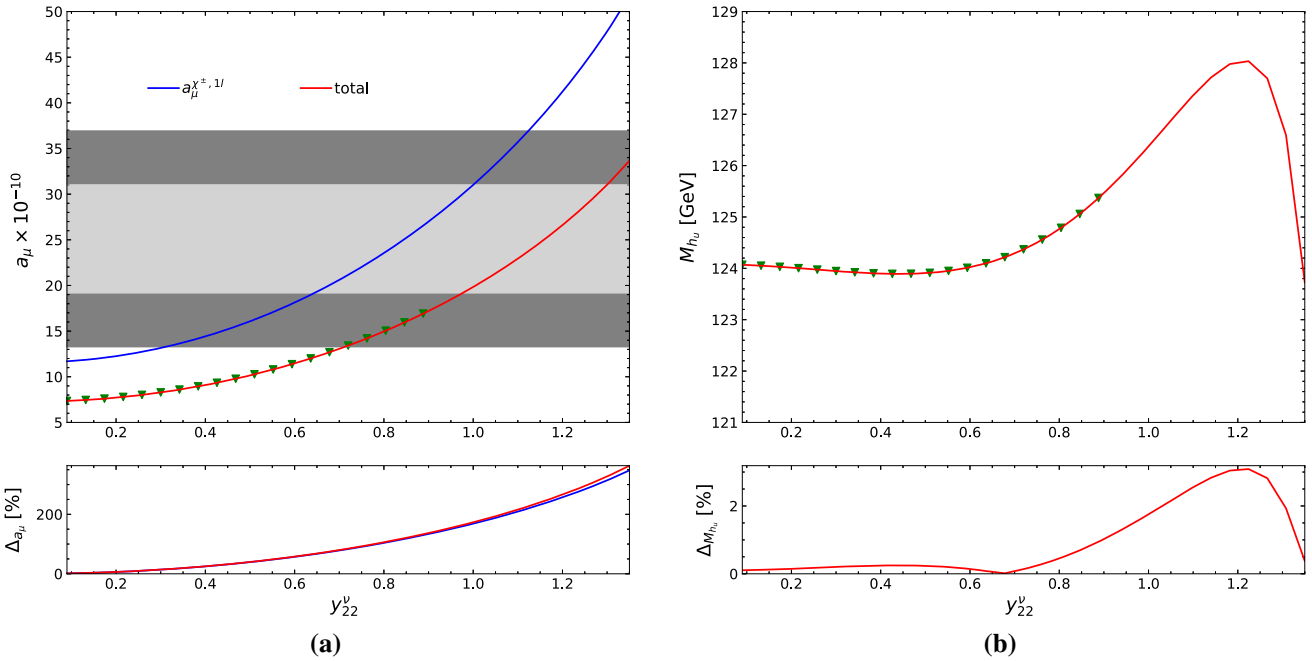

Fig. 2 Upper left: The one-loop chargino contribution (blue) and the sum of all contributions (red) to the AMM of the muon in the NMSSM-nuSS. Lower left: The corresponding relative difference defined as $\Delta_{a_\mu} = \left|(a_\mu^x(\text{NMSSM-nuSS}) - a_\mu^x(\text{NMSSM}))/a_\mu^x(\text{NMSSM})\right|$. Both as a function of y_{22}^ν in the M_X parameterization. Upper right: The loop-corrected mass of the h_u-like Higgs boson in GeV at order $\mathcal{O}(\alpha_t\alpha_s + \alpha_t^2)$. Lower right: The corresponding relative difference $\Delta_{M_{h_u}} = \left|(M_{h_u}^{\text{NMSSM-nuSS}} - M_{h_u}^{\text{NMSSM}})/M_{h_u}^{\text{NMSSM}}\right|$. Both as a function of y_{22}^ν in the μ_X parameterization

tract the W-boson SM contribution from the W-boson contribution in the NMSSM-nuSS as mentioned in Sect. 3.1. In the NMSSM without ISS, the W-boson contribution is exactly equal to the SM one, that is why it does not appear in Table 3. To understand better the W-boson contribution in the NMSSM-nuSS, we look at the neutrino spectrum. For this particular point μ_X has been set to 600 GeV, so that there are four sterile neutrinos, two with a mass of about 600 GeV and two with mass around 619 GeV. We have tried to reduce μ_X to decrease the sterile neutrino masses so that the magnitude of the W-boson contribution increases. But this also leads to the violation of the unitarity constraint, see [31] for the definition of this constraint. The magnitude of the charged Higgs contribution has increased by a factor of about 10^5 compared to the NMSSM without ISS. This is because in the NMSSM without ISS, the charged Higgs contribution is suppressed by the factor m_l^4/v^2 while in the model with ISS there appears a new contribution being proportional to $m_l^2 y_{ll}^\nu$, see (39). This contribution can be $\mathcal{O}(10^{-10})$ if the charged Higgs mass is light enough. For our parameter point, the charged Higgs mass is 1 TeV, so that its contribution is of $\mathcal{O}(10^{-11})$ which does not play an important role in the sum of all contributions.

Comparison with the impact on the SM-like Higgs mass: We now investigate the impact of the neutrino and sneutrino parameters on the muon AMM in the NMSSM-nuSS in comparison to their impact on the SM-like Higgs boson mass. Starting from the parameter point `P1`, we have varied several parameters to see the change of the sum of all contributions a_μ to the AMM. We can divide them into two sets. The first set contains parameters that change the muon-neutrino Yukawa coupling y_{22}^ν. It enters directly the couplings of the W boson, the charged Higgs and the chargino with neutrinos. In the μ_X parameterization, it is y_{22}^ν that is changed, while in the Casas–Ibarra parameterization it is μ_X and λ_X that are changed. The second set includes parameters that result in a significant change of the spectrum of the sneutrino masses. The sneutrino trilinear coupling A_{22}^ν, A_{22}^X, and

the soft SUSY-breaking masses $\tilde{m}^X_{22}$, $\tilde{m}^N_{22}$, $B^{\mu_X}_{22}$ belong to the second set.

In Fig. 2 we vary y^ν_{22} in the range [0.9, 1.35], keeping the other parameters fixed as in the parameter point P1 using the μ_X parameterization. If $y^\nu_{22} > 1.45$, one enters the region where the sneutrino mass squared becomes negative. We remind the reader that y^ν_{22} enters the couplings between the muon, the charginos and the sneutrinos and also enters the mass matrix of the sneutrinos. Increasing y^ν_{22} leads to an increase of the mixing between the left-handed muon sneutrinos $\tilde{\nu}_2$, $\tilde{N}_2$, $\tilde{X}_2$, so that the mass of the $\tilde{\nu}_2$-like sneutrino becomes smaller while the mass of the $\tilde{N}_2$-like sneutrino increases. In the upper left plot, we show the dependence of the one-loop chargino contribution (blue) and the sum of all contributions (red) to the AMM of the muon in the NMSSM-nuSS as a function of y^ν_{22}. We see a strong dependence on y^ν_{22} which can be understood by using an approximate expression for the new contribution from the one-loop chargino contribution in the NMSSM-nuSS. New contribution here means the difference between the one-loop chargino contribution in the NMSSM-nuSS and in the NMSSM. It can be obtained by using the mass insertion method. The Feynman diagram in Fig. 3 exemplifies the enhancement mechanism. In the region of large y^ν_{22}, the approximate new contribution is given by

$$\begin{aligned} a_\mu^{\chi^\pm,1l}(\text{new}) \sim & -\frac{m_l}{8\pi^2}(y^\nu_{22})^2 y_\mu \frac{\mu^2_{\text{eff}} v \text{Re}(s_\beta A^\nu_{22} e^{i\varphi_u} - c_\beta \mu_{\text{eff}})}{(M_{\tilde{\nu}_+\tilde{\nu}_+})_{22} - (M_{\tilde{N}_+\tilde{N}_+})_{22}} \\ & \times (D_1((M_{\tilde{\nu}_+\tilde{\nu}_+})_{22}, \mu^2_{\text{eff}}, \mu^2_{\text{eff}}, \mu^2_{\text{eff}}) \\ & - D_1((M_{\tilde{N}_+\tilde{N}_+})_{22}, \mu^2_{\text{eff}}, \mu^2_{\text{eff}}, \mu^2_{\text{eff}})), \end{aligned} \tag{96}$$

where D_1 denotes the rank-1 four-point function where all external momenta are set equal to zero,

$$D_1(x, y, y, y) = -\frac{(2x^2 + 5xy - y^2)}{12(x-y)^3 y} + \frac{x^2 \log(x/y)}{2(x-y)^4}, \tag{97}$$

and $(M_{\tilde{\nu}_+\tilde{\nu}_+})_{22}$, $(M_{\tilde{N}_+\tilde{N}_+})_{22}$ are the second diagonal components of the sneutrino mass matrix, see Appendix A. This contribution is proportional to $(y^\nu_{22})^2$ in which one factor y^ν_{22} arises from the coupling $\tilde{H}_u \mu \tilde{N}$ and the other comes from the mixing between $\tilde{\nu}$ and $\tilde{N}$. In the upper left plot Fig. 2, we also highlighted the 1σ (light gray) and the 2σ (dark gray) regions of the difference between the experimental value and the SM prediction as defined in (4). The points denoted by green triangles are those points that pass all our constraints. In the lower left plot of Fig. 2 we show the relative difference between the muon AMM in the two models NMSSM and NMSSM-nuSS, defined as

$$\Delta_{a_\mu} = \left| \frac{(a^x_\mu(\text{NMSSM-nuSS}) - a^x_\mu(\text{NMSSM}))}{a^x_\mu(\text{NMSSM})} \right|, \tag{98}$$

where x can be the chargino one-loop contribution or the sum of all contributions. The relative difference is dominated by the chargino one-loop contribution and strongly increases with y^ν_{22} from 0 to more than 350% in the range of the y^ν_{22} variation. In the upper right plot of Fig. 2 we show the variation of the loop-corrected Higgs boson mass for the h_u-like state at order $\mathcal{O}(\alpha_t\alpha_s + \alpha_t^2)$ as a function of y^ν_{22}. As can be inferred from the plot, in the region $y^\nu_{22} > 0.65$ the neutrino/sneutrino sector strongly affects the mass of the h_u-like Higgs boson. It increases until y^ν_{22} reaches 1.2 and then quickly decreases. This is due to the interplay between the positive contributions from the neutrino one-loop diagrams and the negative contributions from the sneutrino one-loop diagrams. The variation of y^ν_{22} affects both contributions simultaneously. At large y^ν_{22} the sneutrino mass becomes very small so that its effect gets stronger than the neutrino one and it reduces the mass M_{h_u} of the h_u-like Higgs boson to a very small value. The relative difference between the h_u-like Higgs boson mass in the NMSSM-nuSS and the NMSSM as function of y^ν_{22} is shown in the lower right plot of Fig. 2. From small values it increases starting from $y^\nu_{22} = 0.65$ until it reaches a maximum of 3% at 1.2 and decreases again to small relative differences.

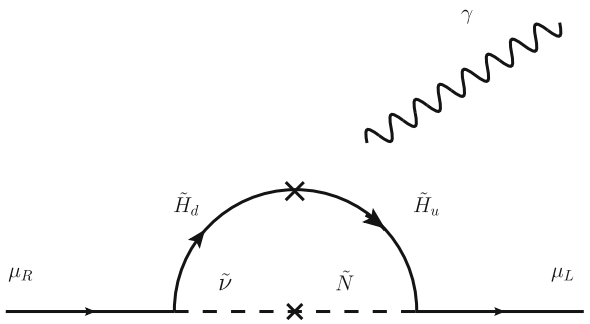

Fig. 3 The new enhancement mechanism contributing to the anomalous magnetic moment of the muon in the NMSSM-nuSS

Dependence on A^ν_{22}: The dependence of the muon AMM and the loop-corrected h_u-like Higgs boson mass on the magnitude of the neutrino soft SUSY-breaking trilinear coupling A^ν_{22} is presented in Fig. 4. We varied A^ν_{22} in the range $[-1400, 1400]$ GeV. The notation and color code is the same as in Fig. 2. The nearly linear dependence of the chargino one-loop contribution seen in Fig. 4 (upper left) can be explained by using the approximate expression in (96). The change of the sign of the new contribution around $A^\nu_{22} \sim 0$ can be seen in the lower left plot of Fig. 4. For the explanation of the experimental result for $(g-2)_\mu$ a negative value of A^ν_{22} is preferred. This feature gives also a possibility for the NMSSM-nuSS to explain simultaneously both the positive discrepancy in $(g-2)_\mu$ and the negative discrepancy in $(g-2)_e$ [65–67] by choosing a negative value for A^ν_{22} and a positive value for A^ν_{11} as shown in [35]. For the parameter point P1, it is impossible to obtain the SUSY contributions for the electron AMM of -7×10^{-13} to be close to the deviation between

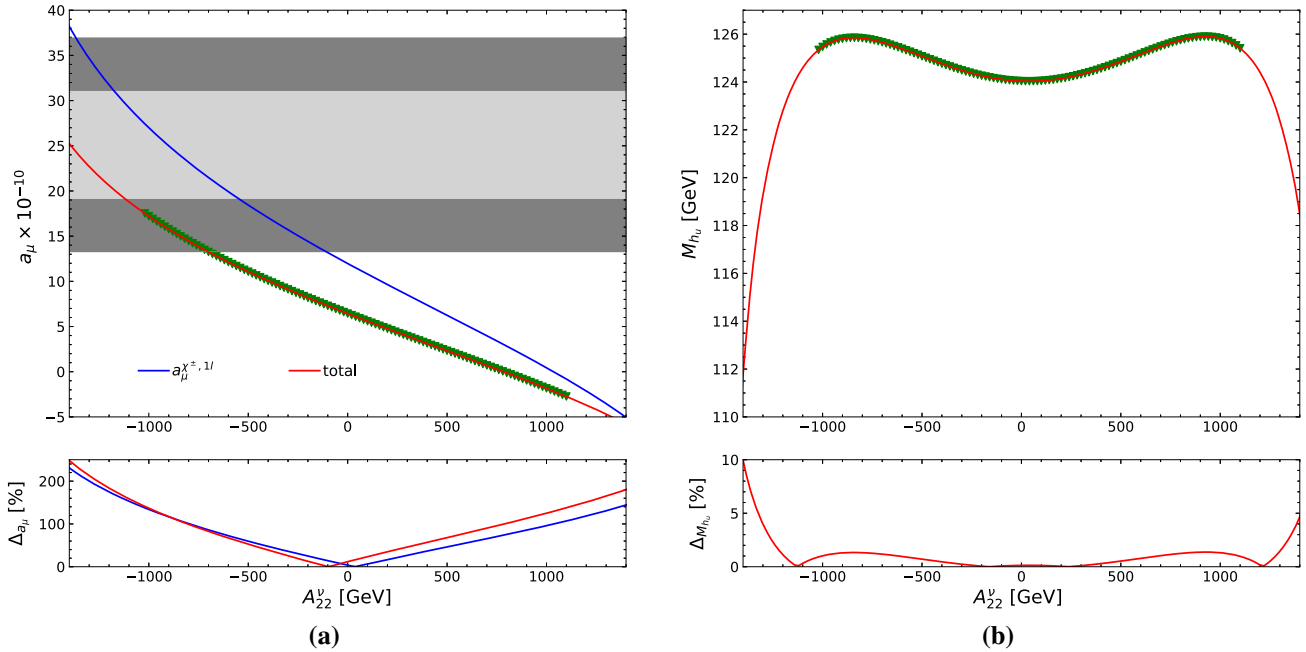

Fig. 4 Similar to Fig. 2 but now A_{22}^ν is varied instead

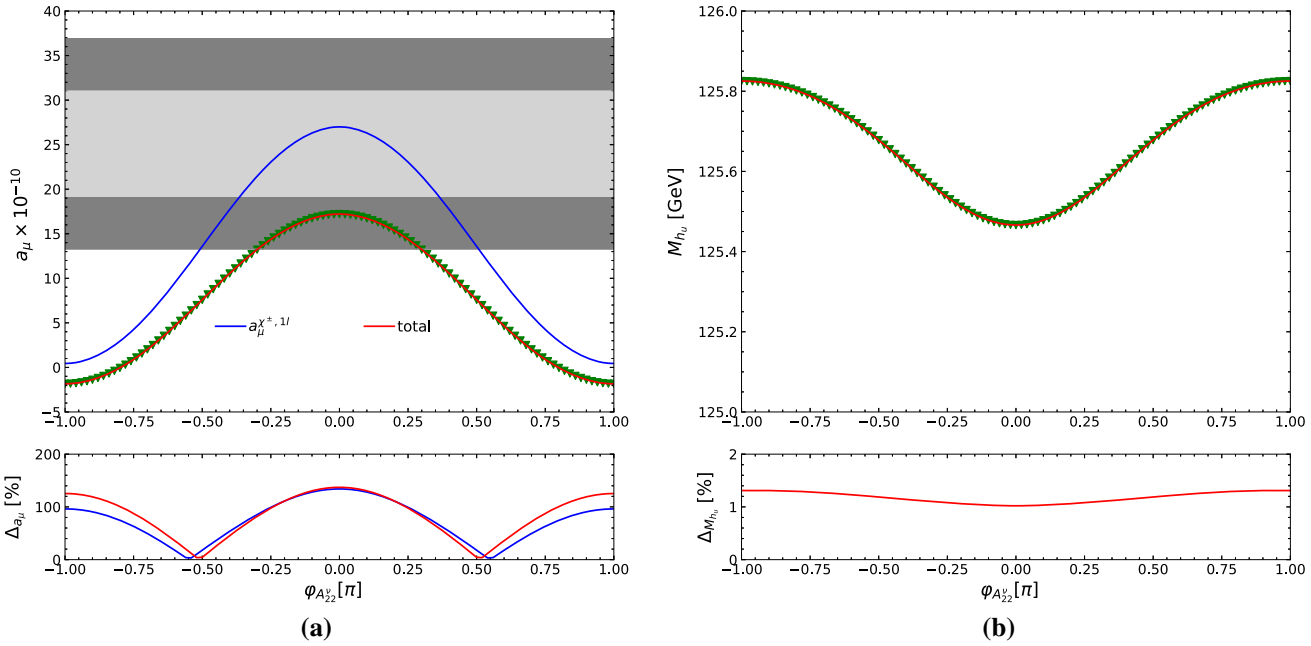

Fig. 5 Effect of the complex phase of A_{22}^ν on the AMM of the muon (left) and the loop-corrected mass of the h_u-like Higgs boson. The color code is the same as Fig. 2

the experimental measurement and the SM prediction while it still satisfies other constraints. In the right plots of Fig. 4, we can see the dependence of the loop-corrected h_u-like Higgs boson mass on A_{22}^ν in the upper plot while in the lower plot we see the relative difference of this mass in the two models with and without inverse seesaw mechanism. The larger the magnitude of A_{22}^ν is, the larger the mixing between $\tilde{\nu}$ and $\tilde{N}$ becomes. This leads to the reduction of the mass of the left-handed muon-like sneutrino. As a consequence the sneutrino contributions become dominant compared to the neutrino contributions.

Influence of the CP-violating phases: We now discuss the influence of the CP-violating phases on the muon AMM and the loop-corrected h_u-like Higgs boson mass. In Fig. 5, we

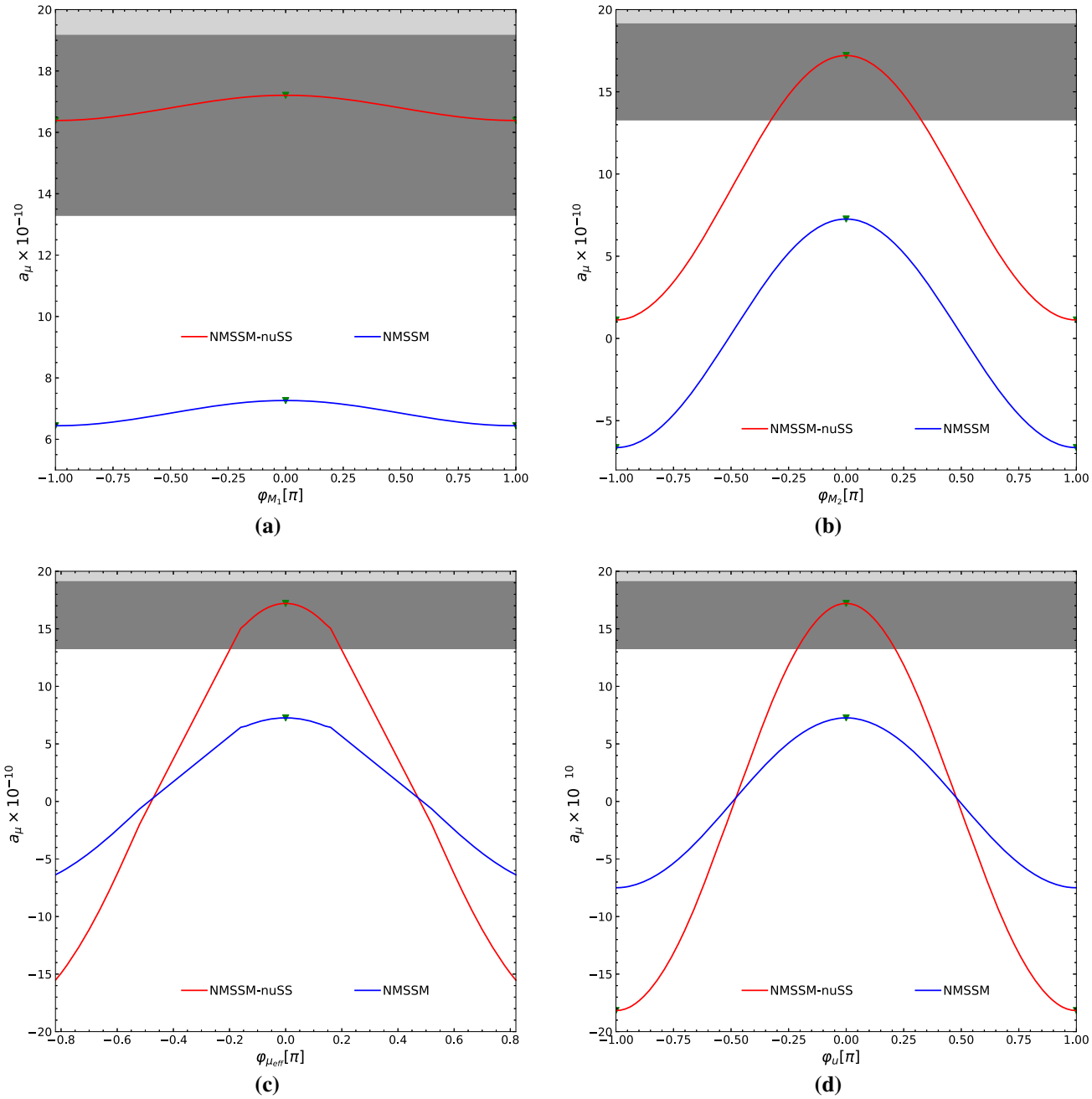

Fig. 6 The AMM of the muon in the NMSSM with (red) and without (blue) inverse seesaw mechanism as a function of several CP-violating phases: **a** φ_{M_1}, **b** φ_{M_2}, **c** $\varphi_{\mu_{\rm eff}}$, **d** φ_u

vary the complex phase of A^{ν}_{22} in the range $[-\pi, \pi]$. The SUSY contributions to a_μ change its value from -2×10^{-10} at $\varphi_{A^{\nu}_{22}} = -\pi$ to reach a maximum of 17.2×10^{-10} at $\varphi_{A^{\nu}_{22}} = 0$ and then reduce it back to -2×10^{-10} at $\varphi_{A^{\nu}_{22}} = \pi$. While the complex phase of A^{ν}_{22} strongly affects the $(g-2)_\mu$, its effect on the mass of the h_u-like Higgs boson is rather mild as can seen in the right plots of Fig. 5. We further present in Fig. 6 the influence of several complex phases, namely $\varphi_{M_1}, \varphi_{M_2}, \varphi_{\mu_{\rm eff}}, \varphi_u$, on the SUSY contributions to a_μ in both models, the NMSSM with and without inverse seesaw mechanism. In all these plots, the NMSSM-nuSS results are plotted in red while the blue lines show the results in the NMSSM without inverse seesaw mechanism. The complex phase of M_1 enters only the neutralino contribution. Figure 6a shows a mild dependence of $(g-2)_\mu$ on this phase for this particular point where the neutralino contribution is always negative and about four times smaller than the dominant chargino contribution. The complex phase of M_2 enters

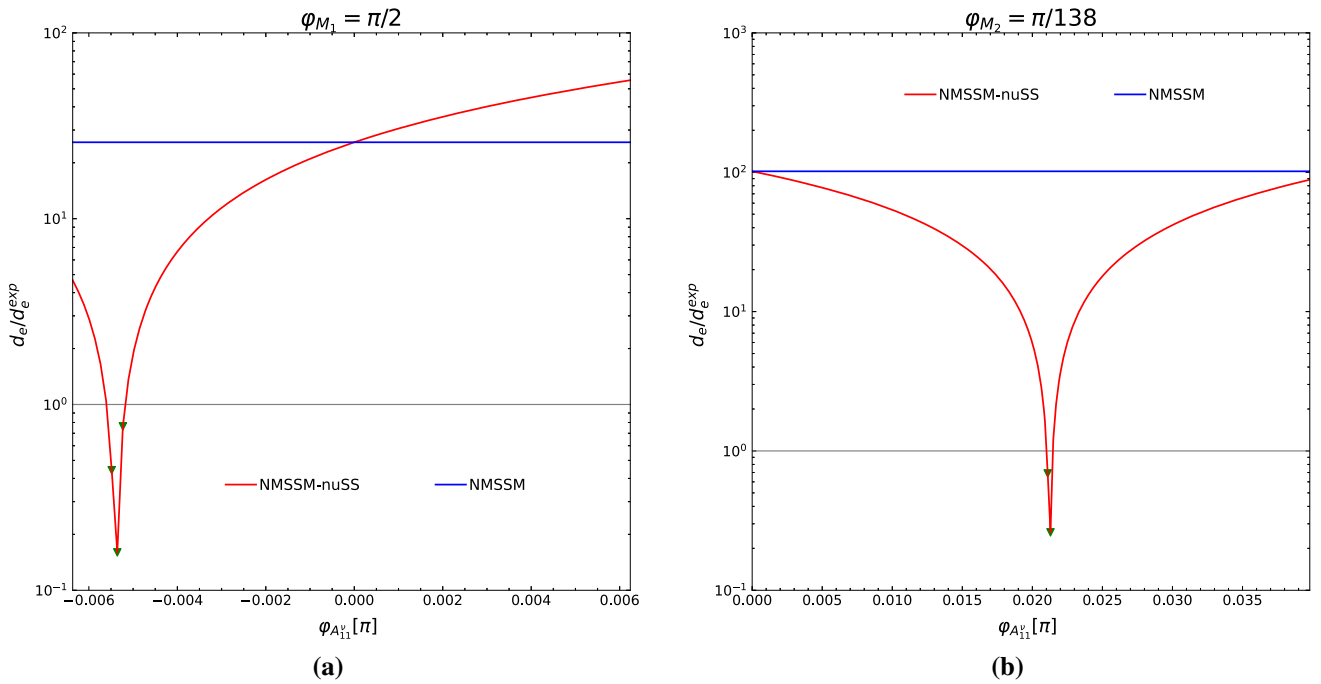

Fig. 7 The EDM of the electron in the NMSSM with (red) and without (blue) inverse seesaw mechanism as a function of the complex phase of A_{11}^ν where **a** $\varphi_{M_1} = \pi/2$, **b** $\varphi_{M_2} = \pi/138$

not only the neutralino contribution but also the chargino one. In Fig. 6b we can see a similar dependence of $(g-2)_\mu$ on this phase in both models. The two remaining phases $\varphi_{\mu_{\text{eff}}}$ and φ_u have a stronger influence on $(g-2)_\mu$ in the NMSSM-nuSS than in the NMSSM without ISS as shown in Fig. 6c, d. This is due to these two phases entering the new contribution in the NMSSM-nuSS, see (96). Note that in Fig. 6c the range of $\varphi_{\mu_{\text{eff}}}$ is $[-0.8\pi, 08\pi]$ since outside this range the mass of the h_u-like Higgs boson turns out to be negative. For illustrative purpose we show partly the light gray and dark gray regions representing the 1σ and 2σ deviations between the experimental measurement and the SM prediction for $(g-2)_\mu$. In these plots, except for the points where the phases $\varphi_{M_1}, \phi_{M_2}, \varphi_{\mu_{\text{eff}}}, \varphi_u$ are close to zero or $\pm\pi$, all other points are ruled out because of the constraints on the electric dipole moments of the electron.

Effects on the electron EDM: We now investigate the effect of the new complex phase in the (s)neutrino sectors on the electron EDM. In NMSSMCALC, the electron, neutron, Thallium and Mercury EDMs have been implemented as described in [47]. We follow the conventions in NMSSMCALC that all EDMs are normalized to their corresponding experimental upper bounds. A thorough investigation of the complex phases in the NMSSM on the electron, neutron, Thallium and Mercury EDMs in [47] has shown that the complex phases of the electroweak sector such as $\varphi_{M_1}, \varphi_{M_2}$, $\varphi_1 \equiv \varphi_\lambda + \varphi_s + \varphi_u, \varphi_2 \equiv \varphi_\kappa + 3\varphi_s$ have the strongest effects on the electron EDM which also enters the Thallium and Mercury EDMs. These phases contribute to the electron EDM through the one-loop neutralino and chargino contributions as can be inferred from the second terms in (41) and (40). Apart from the NMSSM-like phase φ_2, the stringent limit on the electron EDM has ruled out almost any non-vanishing value of these complex phases as we also observe in this study (see previous paragraph). In the NMSSM-nuSS, there are new complex phases from the neutrino sector, $\delta_{CP}, \varphi_{y_{11}^\nu}, \varphi_{\mu_{11}^X}, \varphi_{\lambda_{11}^X}$, and from the sneutrino sector $\varphi_{A_{11}^\nu}, \varphi_{A_{11}^X}, \varphi_{B_{11}^{\mu_X}}$. However, only the complex phase $\varphi_{A_{11}^\nu}$ gives a significant contribution to the EDMs, all other remaining phases have a negligible effect. The complex phase $\varphi_{A_{11}^\nu}$ appears in the one-loop chargino contribution, see the second term in (40). This provides a possibility for the reduction of the imaginary part of the coupling $g^R_{l\tilde{\chi}_j^-\tilde{\nu}_i}$, see (44), and may thereby lead to the cancellation between different contributions to the electron EDM. Such a cancellation can never happen in the NMSSM without ISS.

To illustrate this, we show in Fig. 7 the dependence of the electron EDM, normalized to the experimental upper bound, on the complex phase of A_{11}^ν using the parameter point P1. In the left plot, we have set $\varphi_{M_1} = \pi/2$ while in the right plot we have set $\varphi_{M_2} = \pi/138$. All other phases are equal to zero. These values of φ_{M_1} and φ_{M_2} correspond to the largest possible induced EDM of the neutron from the respective phases that still remains below the experimental upper bound. The red (blue) lines show the electron EDMs in the NMSSM with (without) ISS. As can be inferred from the plots, in the

NMSSM without ISS the electron EDM is about 25 times larger than its experimental upper bound for $\varphi_{M_1} = \pi/2$ and about 102 times larger for $\varphi_{M_2} = \pi/138$. In the NMSSM with ISS a cancellation of all contributions to the electron EDM takes place at $\varphi_{A^{\nu}_{11}} = -0.0055\pi$ for $\varphi_{M_1} = \pi/2$ and at $\varphi_{A^{\nu}_{11}} = 0.022\pi$ for $\varphi_{M_2} = \pi/138$ so that the electron EDM is pushed below its experimental upper bound. Note that all the points with the electron EDM being less than one satisfy all our constraints mentioned in this paper. A similar cancellation can also happen for the phases φ_1 and φ_2.

5 Conclusions

In this paper we have computed the full one-loop SUSY contributions and the two-loop Barr–Zee-type diagrams with $h\gamma\gamma$ effective couplings to the AMM and EDM of charged leptons in two models, the NMSSM with and without inverse seesaw mechanism including CP-violating phases. We presented the analytic expressions and implemented them in the two Fortran codes `NMSSMCALC` and `NMSSMCALC-nuSS`, which compute the Higgs boson masses and mixings, together with the Higgs boson decay branching ratios taking into account the most up-to-date higher-order corrections. Using a typical parameter point with an intermediate value of $\tan\beta$ and large charged Higgs mass, we have investigated in the NMSSM with inverse seesaw mechanism the effect of the (s)neutrino sector on the muon AMM in comparison with its effect on the SM-like Higgs-boson mass. We see a large positive contribution to the AMM from the mixing between the left-handed muon-type sneutrino and the right-handed one (denoted as $\tilde{N}$ in the previous sections) provided that the muon-type neutrino Yukawa coupling is of order $\mathcal{O}(1)$, that the muon-type neutrino trilinear coupling is negative and that the left- and right-handed muon-type sneutrino masses are small. Too light sneutrino masses, however, give a large negative correction to the Higgs boson masses. In order to compensate this negative effect one should also require light sterile neutrino masses. Therefore, there is a strong correlation between the effects of the (s)neutrino sector on the two observables. We have also found a strong effect of the CP-violating phases on the AMM of the muon in the two models.

For the electron EDM we found that the complex phase of the sneutrino sector $\varphi_{A^{\nu}_{11}}$ gives a significant contribution at one-loop level. This provides a possibility for the cancellation of the different contributions to the electron EDM so that it remains below the experimental upper bound. While most of the non-vanishing complex phases of the electroweak sector of the NMSSM have been ruled out by the constraint on the electron EDM, in the NMSSM-nuSS one can remain in the region of validity with an appropriately chosen value of $\varphi_{A^{\nu}_{11}}$.

Finally, the calculations presented in this paper have been implemented in the programs `NMSSMCALC` and `NMSSMCALC-nuSS` which are publicly available.

Acknowledgements T.N.D and D.N.L are funded by the Vietnam National Foundation for Science and Technology Development (NAFOSTED) under Grant number 103.01-2020.17. The research of MM was supported by the Deutsche Forschungsgemeinschaft (DFG, German Research Foundation) under Grant 396021762-TRR 257.

Data Availability Statement This manuscript has no associated data or the data will not be deposited. [Authors' comment: The work presented in this paper does not use any experimental data which needs to be deposited. The input parameters are given in the paper and all the numerical results are either given in the tables or displayed in the figures.]

Open Access This article is licensed under a Creative Commons Attribution 4.0 International License, which permits use, sharing, adaptation, distribution and reproduction in any medium or format, as long as you give appropriate credit to the original author(s) and the source, provide a link to the Creative Commons licence, and indicate if changes were made. The images or other third party material in this article are included in the article's Creative Commons licence, unless indicated otherwise in a credit line to the material. If material is not included in the article's Creative Commons licence and your intended use is not permitted by statutory regulation or exceeds the permitted use, you will need to obtain permission directly from the copyright holder. To view a copy of this licence, visit http://creativecommons.org/licenses/by/4.0/.
Funded by SCOAP^3. SCOAP^3 supports the goals of the International Year of Basic Sciences for Sustainable Development.

Appendix A: The sneutrino mass matrix

Here we provide the mass matrix of the sneutrinos. Each entry is a 3×3 matrix in the flavor space.

$$(M_{\tilde{\nu}})_{\tilde{\nu}_+\tilde{\nu}_+} = \frac{1}{2} I_3 M_z^2 \cos 2\beta + \frac{1}{2}\left(\tilde{m}_L^2 + \tilde{m}_L^{2T}\right) + \frac{1}{2} v_u^2 \mathrm{Re}\left(y_\nu y_\nu^\dagger\right) \tag{99}$$

$$(M_{\tilde{\nu}})_{\tilde{\nu}_+\tilde{N}_+} = \frac{1}{\sqrt{2}} v_u \mathrm{Re}\left(e^{i\varphi_u} y_\nu A_\nu\right) - \frac{1}{2} v_d v_s \mathrm{Re}\left(e^{i\varphi_s} \lambda y_\nu^*\right) \tag{100}$$

$$(M_{\tilde{\nu}})_{\tilde{\nu}_+\tilde{X}_+} = \frac{1}{\sqrt{2}} v_u \mathrm{Re}\left(e^{i\varphi_u} y_\nu \mu_X^*\right) \tag{101}$$

$$(M_{\tilde{\nu}})_{\tilde{\nu}_+\tilde{\nu}_-} = \frac{i}{2}\left(\tilde{m}_L^2 - \tilde{m}_L^{2T}\right) + \frac{1}{2} v_u^2 \mathrm{Im}\left(y_\nu y_\nu^\dagger\right) \tag{102}$$

$$(M_{\tilde{\nu}})_{\tilde{\nu}_+\tilde{N}_-} = \frac{1}{\sqrt{2}} v_u \mathrm{Im}\left(e^{i\varphi_u} y_\nu A_\nu\right) - \frac{1}{2} v_d v_s \mathrm{Im}\left(e^{i\varphi_s} \lambda y_\nu^*\right) \tag{103}$$

$$(M_{\tilde{\nu}})_{\tilde{\nu}_+\tilde{X}_-} = \frac{1}{\sqrt{2}} v_u \mathrm{Im}\left(e^{i\varphi_u} y_\nu \mu_X^*\right) \tag{104}$$

$$(M_{\tilde{\nu}})_{\tilde{N}_+\tilde{N}_+} = \frac{1}{2}\left(\tilde{m}_N^2 + \tilde{m}_N^{2T}\right) + \mathrm{Re}\left(\mu_X \mu_X^\dagger\right) + \frac{1}{2} v_u^2 \mathrm{Re}\left(y_\nu^T y_\nu^*\right) \tag{105}$$

$$(M_{\tilde{\nu}})_{\tilde{N}_+\tilde{X}_+} = \mathrm{Re}\left(\mu_X B_{\mu_X}\right) + \frac{1}{\sqrt{2}} v_s \mathrm{Re}\left[e^{-i\varphi_s}\mu_X\left(\lambda_X^\dagger + \lambda_X^*\right)\right] \tag{106}$$

$$(M_{\tilde{\nu}})_{\tilde{N}_+\tilde{\nu}_-} = -\frac{1}{\sqrt{2}} v_u \mathrm{Im}\left(e^{i\varphi_u} A_\nu^T y_\nu^T\right) - \frac{1}{2} v_d v_s \mathrm{Im}\left(e^{i\varphi_s}\lambda y_\nu^\dagger\right) \tag{107}$$

$$(M_{\tilde{\nu}})_{\tilde{N}_+\tilde{N}_-} = \frac{i}{2}\left(\tilde{m}_N^2 - \tilde{m}_N^{2T}\right) - \mathrm{Im}\left(\mu_X \mu_X^\dagger\right) - \frac{1}{2} v_u^2 \mathrm{Im}\left(y_\nu^T y_\nu^*\right) \tag{108}$$

$$(M_{\tilde{\nu}})_{\tilde{N}_+\tilde{X}_-} = -\mathrm{Im}\left(\mu_X B_{\mu_X}\right) + \frac{1}{\sqrt{2}} v_s \mathrm{Im}\left[e^{-i\varphi_s}\mu_X\left(\lambda_X^\dagger + \lambda_X^*\right)\right] \tag{109}$$

$$\begin{aligned}(M_{\tilde{\nu}})_{\tilde{X}_+\tilde{X}_+} = {} & \frac{1}{2}\left(\tilde{m}_X^2 + \tilde{m}_X^{2T}\right) + \mathrm{Re}\left(\mu_X^T \mu_X^*\right) \\ & + \frac{1}{2}\mathrm{Re}\left[\left(e^{2i\varphi_s} v_s^2 \kappa - e^{i\varphi_u} v_d v_u \lambda\right)\left(\lambda_X^* + \lambda_X^\dagger\right)\right] \\ & + \frac{1}{2} v_s^2 \mathrm{Re}\left[\left(\lambda_X + \lambda_X^T\right)\left(\lambda_X^\dagger + \lambda_X^*\right)\right] \\ & + \frac{1}{\sqrt{2}} v_s \mathrm{Re}\left[e^{i\varphi_s}\left(\lambda_X A_X + A_X^T \lambda_X^T\right)\right]\end{aligned} \tag{110}$$

$$(M_{\tilde{\nu}})_{\tilde{X}_+\tilde{\nu}_-} = -\frac{1}{\sqrt{2}} v_u \mathrm{Im}\left(e^{i\varphi_u}\mu_X^\dagger y_\nu^T\right) \tag{111}$$

$$\begin{aligned}(M_{\tilde{\nu}})_{\tilde{X}_+\tilde{N}_-} = {} & \mathrm{Im}\left(B_{\mu_X}^T \mu_X^T\right) \\ & + \frac{1}{\sqrt{2}} v_s \mathrm{Im}\left[e^{-i\varphi_s}\left(\lambda_X^\dagger + \lambda_X^*\right)\mu_X^T\right]\end{aligned} \tag{112}$$

$$\begin{aligned}(M_{\tilde{\nu}})_{\tilde{X}_+\tilde{X}_-} = {} & \frac{i}{2}\left(\tilde{m}_X^2 - \tilde{m}_X^{2T}\right) + \mathrm{Im}\left(\mu_X^T \mu_X^*\right) \\ & + \frac{1}{2}\mathrm{Im}\left[\left(e^{2i\varphi_s} v_s^2 \kappa - e^{i\varphi_u} v_d v_u \lambda\right)\left(\lambda_X^* + \lambda_X^\dagger\right)\right] \\ & + \frac{1}{2} v_s^2 \mathrm{Im}\left[\left(\lambda_X + \lambda_X^T\right)\left(\lambda_X^\dagger + \lambda_X^*\right)\right] \\ & - \frac{1}{\sqrt{2}} v_s \mathrm{Im}\left[e^{i\varphi_s}\left(\lambda_X A_X + A_X^T \lambda_X^T\right)\right]\end{aligned} \tag{113}$$

$$(M_{\tilde{\nu}})_{\tilde{\nu}_-\tilde{\nu}_-} = \frac{1}{2} I_3 M_z^2 \cos 2\beta + \frac{1}{2}\left(\tilde{m}_L^2 + \tilde{m}_L^{2T}\right) + \frac{1}{2} v_u^2 \mathrm{Re}\left(y_\nu y_\nu^\dagger\right) \tag{114}$$

$$(M_{\tilde{\nu}})_{\tilde{\nu}_-\tilde{N}_-} = \frac{1}{\sqrt{2}} v_u \mathrm{Re}\left(e^{i\varphi_u} y_\nu A_\nu\right) - \frac{1}{2} v_d v_s \mathrm{Re}\left(e^{i\varphi_s}\lambda y_\nu^*\right) \tag{115}$$

$$(M_{\tilde{\nu}})_{\tilde{\nu}_-\tilde{X}_-} = \frac{1}{\sqrt{2}} v_u \mathrm{Re}\left(e^{i\varphi_u} y_\nu \mu_X^*\right) \tag{116}$$

$$(M_{\tilde{\nu}})_{\tilde{N}_-\tilde{N}_-} = \frac{1}{2}\left(\tilde{m}_N^2 + \tilde{m}_N^{2T}\right) + \mathrm{Re}\left(\mu_X \mu_X^\dagger\right) + \frac{1}{2} v_u^2 \mathrm{Re}\left(y_\nu^T y_\nu^*\right) \tag{117}$$

$$(M_{\tilde{\nu}})_{\tilde{N}_-\tilde{X}_-} = \mathrm{Re}\left(\mu_X B_{\mu_X}\right) - \frac{1}{\sqrt{2}} v_s \mathrm{Re}\left[e^{-i\varphi_s}\mu_X\left(\lambda_X^\dagger + \lambda_X^*\right)\right] \tag{118}$$

$$\begin{aligned}(M_{\tilde{\nu}})_{\tilde{X}_-\tilde{X}_-} = {} & \frac{1}{2}\left(\tilde{m}_X^2 + \tilde{m}_X^{2T}\right) + \mathrm{Re}\left(\mu_X^T \mu_X^*\right) \\ & - \frac{1}{2}\mathrm{Re}\left[\left(e^{2i\varphi_s} v_s^2 \kappa - e^{i\varphi_u} v_d v_u \lambda\right)\left(\lambda_X^* + \lambda_X^\dagger\right)\right] \\ & + \frac{1}{2} v_s^2 \mathrm{Re}\left[\left(\lambda_X + \lambda_X^T\right)\left(\lambda_X^\dagger + \lambda_X^*\right)\right] \\ & - \frac{1}{\sqrt{2}} v_s \mathrm{Re}\left[e^{i\varphi_s}\left(\lambda_X A_X + A_X^T \lambda_X^T\right)\right].\end{aligned} \tag{119}$$

References

1. Muon g-2 Collaboration, B. Abi et al., Measurement of the positive muon anomalous magnetic moment to 0.46 ppm. Phys. Rev. Lett. **126**, 141801 (2021). arXiv:2104.03281
2. Muon g-2 Collaboration, G.W. Bennett et al., Final report of the muon E821 anomalous magnetic moment measurement at BNL. Phys. Rev. D **73**, 072003 (2006). arXiv:hep-ex/0602035
3. T. Aoyama et al., The anomalous magnetic moment of the muon in the Standard Model. Phys. Rep. **887**, 1–166 (2020). arXiv:2006.04822
4. T. Aoyama, M. Hayakawa, T. Kinoshita, M. Nio, Complete tenth-order QED contribution to the muon g-2. Phys. Rev. Lett. **109**, 111808 (2012). arXiv:1205.5370
5. E.-H. Chao, R.J. Hudspith, A. Gérardin, J.R. Green, H.B. Meyer, K. Ottnad, Hadronic light-by-light contribution to $(g-2)_\mu$ from lattice QCD: a complete calculation. Eur. Phys. J. C **81**, 651 (2021). arXiv:2104.02632
6. A. Czarnecki, W.J. Marciano, The muon anomalous magnetic moment: a harbinger for 'new physics'. Phys. Rev. D **64**, 013014 (2001). arXiv:hep-ph/0102122
7. P. Fayet, Supergauge invariant extension of the Higgs mechanism and a model for the electron and its neutrino. Nucl. Phys. B **90**, 104–124 (1975)
8. R. Barbieri, S. Ferrara, C.A. Savoy, Gauge models with spontaneously broken local supersymmetry. Phys. Lett. B **119**, 343 (1982)
9. M. Dine, W. Fischler, M. Srednicki, A simple solution to the strong CP problem with a harmless axion. Phys. Lett. B **104**, 199 (1981)
10. H.P. Nilles, M. Srednicki, D. Wyler, Weak interaction breakdown induced by supergravity. Phys. Lett. B **120**, 346 (1983)
11. J. Frere, D. Jones, S. Raby, Fermion masses and induction of the weak scale by supergravity. Nucl. Phys. B **222**, 11 (1983)
12. J. Derendinger, C.A. Savoy, Quantum effects and SU(2) x U(1) breaking in supergravity gauge theories. Nucl. Phys. B **237**, 307 (1984)
13. J.R. Ellis, J. Gunion, H.E. Haber, L. Roszkowski, F. Zwirner, Higgs bosons in a nonminimal supersymmetric model. Phys. Rev. D **39**, 844 (1989)
14. M. Drees, Supersymmetric models with extended Higgs sector. Int. J. Mod. Phys. A **4**, 3635 (1989)
15. U. Ellwanger, M. Rausch de Traubenberg, C.A. Savoy, Particle spectrum in supersymmetric models with a gauge singlet. Phys. Lett. B **315**, 331–337 (1993). arXiv:hep-ph/9307322
16. U. Ellwanger, M. Rausch de Traubenberg, C.A. Savoy, Higgs phenomenology of the supersymmetric model with a gauge singlet. Z. Phys. C **67**, 665–670 (1995). arXiv:hep-ph/9502206
17. U. Ellwanger, M. Rausch de Traubenberg, C.A. Savoy, Phenomenology of supersymmetric models with a singlet. Nucl. Phys. B **492**, 21–50 (1997). arXiv:hep-ph/9611251
18. T. Elliott, S. King, P. White, Unification constraints in the next-to-minimal supersymmetric standard model. Phys. Lett. B **351**, 213–219 (1995). arXiv:hep-ph/9406303
19. S. King, P. White, Resolving the constrained minimal and next-to-minimal supersymmetric standard models. Phys. Rev. D **52**, 4183–4216 (1995). arXiv:hep-ph/9505326

20. F. Franke, H. Fraas, Neutralinos and Higgs bosons in the next-to-minimal supersymmetric standard model. Int. J. Mod. Phys. A **12**, 479–534 (1997). arXiv:hep-ph/9512366
21. M. Maniatis, The next-to-minimal supersymmetric extension of the standard model reviewed. Int. J. Mod. Phys. A **25**, 3505–3602 (2010). arXiv:0906.0777
22. U. Ellwanger, C. Hugonie, A.M. Teixeira, The next-to-minimal supersymmetric standard model. Phys. Rep. **496**, 1–77 (2010). arXiv:0910.1785
23. M. Krawczyk, Precision muon g-2 results and light Higgs bosons in the 2HDM(II). Acta Phys. Pol. B **33**, 2621–2634 (2002). arXiv:hep-ph/0208076
24. F. Domingo, U. Ellwanger, Constraints from the muon g-2 on the parameter space of the NMSSM. JHEP **07**, 079 (2008). arXiv:0806.0733
25. R. Mohapatra, Mechanism for understanding small neutrino mass in superstring theories. Phys. Rev. Lett. **56**, 561–563 (1986)
26. R.N. Mohapatra, J.W.F. Valle, Neutrino mass and baryon-number nonconservation in superstring models. Phys. Rev. D **34**, 1642–1645 (1986)
27. J. Bernabeu, A. Santamaria, J. Vidal, A. Mendez, J. Valle, Lepton flavor nonconservation at high-energies in a superstring inspired standard model. Phys. Lett. B **187**, 303–308 (1987)
28. I. Gogoladze, N. Okada, Q. Shafi, NMSSM and seesaw physics at LHC. Phys. Lett. B **672**, 235–239 (2009). arXiv:0809.0703
29. I. Gogoladze, B. He, Q. Shafi, Inverse seesaw in NMSSM and 126 GeV Higgs boson. Phys. Lett. B **718**, 1008–1013 (2013). arXiv:1209.5984
30. W. Wang, J.M. Yang, L.L. You, Higgs boson mass in NMSSM with right-handed neutrino. JHEP **07**, 158 (2013). arXiv:1303.6465
31. T.N. Dao, M. Mühlleitner, A.V. Phan, Loop-corrected Higgs masses in the NMSSM with inverse seesaw mechanism. Eur. Phys. J. C **82**(8), 667 (2022). https://doi.org/10.1140/epjc/s10052-022-10590-9. arXiv:2108.10088 [hep-ph]
32. J. Cao, Y. He, Y. Pan, Y. Yue, H. Zhou, P. Zhu, Impact of leptonic unitarity and dark matter direct detection experiments on the NMSSM with inverse seesaw mechanism. JHEP **12**, 023 (2020). arXiv:1903.01124
33. J. Cao, L. Meng, Y. Yue, H. Zhou, P. Zhu, Suppressing the scattering of WIMP dark matter and nucleons in supersymmetric theories. Phys. Rev. D **101** (7), 075003 (2020). https://doi.org/10.1103/PhysRevD.101.075003. arXiv:1910.14317 [hep-ph]
34. J. Cao, J. Lian, L. Meng, Y. Yue, P. Zhu, Anomalous muon magnetic moment in the inverse seesaw extended next-to-minimal supersymmetric standard model. Phys. Rev. D **101**, 095009 (2020). arXiv:1912.10225
35. J. Cao, Y. He, J. Lian, D. Zhang, P. Zhu, Electron and muon anomalous magnetic moments in the inverse seesaw extended NMSSM. Phys. Rev. D **104**, 055009 (2021). arXiv:2102.11355
36. J. Baglio, R. Gröber, M. Mühlleitner, D. Nhung, H. Rzehak, M. Spira et al., NMSSMCALC: a program package for the calculation of loop-corrected Higgs boson masses and decay widths in the (complex) NMSSM. Comput. Phys. Commun. **185**, 3372–3391 (2014)
37. T. Graf, R. Grober, M. Muhlleitner, H. Rzehak, K. Walz, Higgs boson masses in the complex NMSSM at one-loop level. JHEP **10**, 122 (2012)
38. M. Mühlleitner, D.T. Nhung, H. Rzehak, K. Walz, Two-loop contributions of the order $\mathcal{O}(\alpha_t\alpha_s)$ to the masses of the Higgs bosons in the CP-violating NMSSM. JHEP **05**, 128 (2015). arXiv:1412.0918
39. T. Dao, R. Gröber, M. Krause, M. Mühlleitner, H. Rzehak, Two-loop $\mathcal{O}(\alpha_t^2)$ corrections to the neutral Higgs boson masses in the CP-violating NMSSM. JHEP **08**, 114 (2019)
40. T.N. Dao, M. Gabelmann, M. Mühlleitner, H. Rzehak, Two-loop $\mathcal{O}((\alpha_t + \alpha_\lambda + \alpha_\kappa)^2)$ corrections to the Higgs boson masses in the CP-violating NMSSM. JHEP **09**, 193 (2021). arXiv:2106.06990
41. J.A. Casas, A. Ibarra, Oscillating neutrinos and $\mu \to e\gamma$. Nucl. Phys. B **618**, 171–204 (2001). arXiv:hep-ph/0103065
42. E. Arganda, M.J. Herrero, X. Marcano, C. Weiland, Imprints of massive inverse seesaw model neutrinos in lepton flavor violating Higgs boson decays. Phys. Rev. D **91**, 015001 (2015). arXiv:1405.4300
43. F. Jegerlehner, A. Nyffeler, The muon g-2. Phys. Rep. **477**, 1–110 (2009). arXiv:0902.3360
44. L. Lavoura, General formulae for f(1) → f(2) gamma. Eur. Phys. J. C **29**, 191–195 (2003). arXiv:hep-ph/0302221
45. H.H. Patel, Package-X: a Mathematica package for the analytic calculation of one-loop integrals. Comput. Phys. Commun. **197**, 276–290 (2015). arXiv:1503.01469
46. T. Moroi, The muon anomalous magnetic dipole moment in the minimal supersymmetric standard model. Phys. Rev. D **53**, 6565–6575 (1996). arXiv:hep-ph/9512396
47. S.F. King, M. Muhlleitner, R. Nevzorov, K. Walz, Exploring the CP-violating NMSSM: EDM constraints and phenomenology. Nucl. Phys. B **901**, 526–555 (2015). arXiv:1508.03255
48. C.-H. Chen, C.Q. Geng, The muon anomalous magnetic moment from a generic charged Higgs with SUSY. Phys. Lett. B **511**, 77–84 (2001). arXiv:hep-ph/0104151
49. A. Arhrib, S. Baek, Two loop Barr–Zee type contributions to (g-2)(muon) in the MSSM. Phys. Rev. D **65**, 075002 (2002). arXiv:hep-ph/0104225
50. S. Heinemeyer, D. Stockinger, G. Weiglein, Two loop SUSY corrections to the anomalous magnetic moment of the muon. Nucl. Phys. B **690**, 62–80 (2004). arXiv:hep-ph/0312264
51. S. Heinemeyer, D. Stockinger, G. Weiglein, Electroweak and supersymmetric two-loop corrections to (g-2)(mu). Nucl. Phys. B **699**, 103–123 (2004). arXiv:hep-ph/0405255
52. P. von Weitershausen, M. Schafer, H. Stockinger-Kim, D. Stockinger, Photonic SUSY two-loop corrections to the muon magnetic moment. Phys. Rev. D **81**, 093004 (2010). arXiv:1003.5820
53. H.G. Fargnoli, C. Gnendiger, S. Paßehr, D. Stöckinger, H. Stöckinger-Kim, Non-decoupling two-loop corrections to $(g-2)_\mu$ from fermion/sfermion loops in the MSSM. Phys. Lett. B **726**, 717–724 (2013). arXiv:1309.0980
54. H. Fargnoli, C. Gnendiger, S. Paßehr, D. Stöckinger, H. Stöckinger-Kim, Two-loop corrections to the muon magnetic moment from fermion/sfermion loops in the MSSM: detailed results. JHEP **02**, 070 (2014). arXiv:1311.1775
55. K. Cheung, O.C.W. Kong, J.S. Lee, Electric and anomalous magnetic dipole moments of the muon in the MSSM. JHEP **06**, 020 (2009). arXiv:0904.4352
56. G. Degrassi, G.F. Giudice, QED logarithms in the electroweak corrections to the muon anomalous magnetic moment. Phys. Rev. D **58**, 053007 (1998). arXiv:hep-ph/9803384
57. S.M. Barr, A. Zee, Electric dipole moment of the electron and of the neutron. Phys. Rev. Lett. **65**, 21–24 (1990)
58. T. Abe, J. Hisano, T. Kitahara, K. Tobioka, Gauge invariant Barr–Zee type contributions to fermionic EDMs in the two-Higgs doublet models. JHEP **01**, 106 (2014). arXiv:1311.4704
59. W. Altmannshofer, S. Gori, N. Hamer, H.H. Patel, Phys. Rev. D **102**(11), 115042 (2020). https://doi.org/10.1103/PhysRevD.102.115042. arXiv:2009.01258 [hep-ph]
60. N. Yamanaka, Phys. Rev. D **87**(1), 011701 (2013). https://doi.org/10.1103/PhysRevD.87.011701. arXiv:1211.1808 [hep-ph]
61. P. Bechtle, D. Dercks, S. Heinemeyer, T. Klingl, T. Stefaniak, G. Weiglein et al., HiggsBounds-5: testing Higgs sectors in the LHC 13 TeV era. Eur. Phys. J. C **80**, 1211 (2020). arXiv:2006.06007
62. P. Bechtle, S. Heinemeyer, T. Klingl, T. Stefaniak, G. Weiglein, J. Wittbrodt, HiggsSignals-2: probing new physics with precision Higgs measurements in the LHC 13 TeV era. Eur. Phys. J. C **81**, 145 (2021). arXiv:2012.09197

63. Particle Data Group Collaboration, P. Zyla et al., Review of particle physics. PTEP **2020**, 083C01 (2020)
64. C. Arina, N. Fornengo, JHEP **11**, 029 (2007). https://doi.org/10.1088/1126-6708/2007/11/029. arXiv:0709.4477 [hep-ph]
65. T. Aoyama, T. Kinoshita, M. Nio, Revised and improved value of the QED tenth-order electron anomalous magnetic moment. Phys. Rev. D **97**, 036001 (2018). arXiv:1712.06060
66. D. Hanneke, S. Fogwell, G. Gabrielse, New measurement of the electron magnetic moment and the fine structure constant. Phys. Rev. Lett. **100** 120801 (2008). https://doi.org/10.1103/PhysRevLett.100.120801. arXiv:0801.1134 [physics.atom-ph]
67. D. Hanneke, S. Fogwell Hoogerheide, G. Gabrielse, Cavity control of a single-electron quantum cyclotron: measuring the electron magnetic moment. Phys. Rev. A **83**, 052122 (2011)